SKBF
KBS
TEKNISK
RAPPORT
82-04

Radionuclide chain migration in fissured rock – The influence of matrix diffusion

Anders Rasmuson *
Akke Bengtsson **
Bertil Grunsfelt **
Ivars Neretnieks *
April, 1982

* Royal Institute of Technology
Department of Chemical Engineering
Stockholm, Sweden
** KEMAKTA Consultant Company
Stockholm, Sweden

SVENSK KÄRNBRÄNSLEFÖRSÖRJNING AB / AVDELNING KBS

POSTADRESS: Box 5864, 102 48 Stockholm, Telefon 08-67 95 40

RADIONUCLIDE CHAIN MIGRATION IN FISSURED ROCK - THE INFLUENCE OF MATRIX DIFFUSION

Anders Rasmuson 1)
Akke Bengtsson 2)
Bertil Grundfelt 2)
Ivars Neretnieks 1)

1) Royal Institute of Technology
Department of Chemical Engineering

2) KEMAKTA Consultant Company

Stockholm, Sweden, April 1982

A list of other reports published in this series during 1982, is attached at the end of this report. Information on KBS technical reports from 1977-1978 (TR 121), 1979 (TR 79-28), 1980 (TR 80-26) and 1981 (TR 81-17) is available through SKBF/KBS.

RADIONUCLIDE CHAIN MIGRATION IN FISSURED ROCK - THE INFLUENCE OF MATRIX DIFFUSION

ANDERS RASMUSON 1)

AKKE BENGTSSON 2)

BERTIL GRUNDFELT 2)

IVARS NERETNIEKS 1)

April, 1982

---

1) Department of Chemical Engineering,
Royal Institute of Technology,
S - 100 44 Stockholm, Sweden.

2) KEMAKTA Consultant Company,
Luntmakargatan 94,
S - 113 51 Stockholm, Sweden.

SUMMARY

Diffusion into the rock matrix has a large impact on the migration of radionuclides in the geosphere. The aim of the present study is to investigate the effect of this mechanism on radionuclide chain migration. For this purpose a previously used numerical code TRUMP is extended to incorporate chain decay. The algorithm is also changed to directly include the decay terms. The extended version was given the acronym TRUCHN. Numerical solutions from TRUCHN are compared with the analytical solutions developed by Lester et al. A good agreement is obtained.

To illustrate the impact of matrix diffusion on the arrival times to the biosphere of the members of a radionuclide chain a number of numerical calculations were done for the two chains U-238 → Th-230 → Ra-226 and Pu-239 → U-235 → Pa-231. The resulting curves are compared with the results for surface sorption (penetration depth 10^{-4} m) and volume sorption (complete penetration) obtained with the computer program GETOUT. The differences in first arrival times are very large. The arrival times in the surface and volume sorption cases, differ with as much as four orders of magnitude. The corresponding times for instationary diffusion are located between these extreme values.

A daughter nuclide which is strongly sorbed may be heavily retarded if it is produced far inside the rock matrix and has a long way to diffuse before it reaches the flowing water. This effect is investigated, by considering diffusion only of a radionuclide chain, with analytical and numerical (TRUCHN) methods.

Finally, in connection with the reconcentration effect, some means of describing the outflow of a daughter nuclide in terms of the outflow of its parent nuclide are proposed.

CONTENTS

INTRODUCTION

The migration of radionuclides in fissured rock is strongly affected by diffusion into the rock matrix (Neretnieks, 1980; Rasmuson and Neretnieks, 1981). In the first analysis only one nuclide was considered, and analytic solutions could be derived for simple boundary conditions.

To be able to treat more complicated problems, the numerical model TRUMP (Edwards, 1969) was tested. This code is based on an Integrated Finite Difference Method (Narasimhan and Witherspoon, 1976) and solves the advective diffusion equation in three dimensions, with or without decay and source terms. The program was used to calculate transport of a single radionuclide in fractured rock including advection and longitutinal dispersion in the fractures and diffusion and sorption in the matrix (Rasmuson et al., 1981). Subsequently, the program has been extended so that calculations on radionuclide chain migration can be done. This is described in the present report.

One of the problems specially studied in this paper is the relative movement of mother and daughter nuclides. When several nuclides in a decay chain are considered and the nuclides have different sorption coefficients, a strongly sorbed daughter may be severely hindered if it is born far inside the rock matrix and has a long way to diffuse before it reaches the flowing water.

The other aspect of diffusion into the matrix of a radioactive chain is the so called reconcentration effect. In some cases a daugther may attain an activity considerably higher than the radioactive equilibrium in a closed system. This is a known and studied phenomenon for instantaneous reversible equilibrium but has not been studied yet when matrix diffusion is effective. Another aim of this study was to investigate this effect by sample calculations of the more important chains.

MODIFICATION OF TRUMP

Below is the rationale for extensions to the TRUMP program which enable it to make calculations about radionuclide chain migration. The extended version was given the acronym TRUCHN.

In each time step,calculations for the members in the chain are done in succession, beginning with the first member in the chain. The decay-term for a parent nuclide is a source term for a daugther, and is included as such in the calculation for the daughter. Since the mother nuclide is independent of the daughter nuclide, we may perform n single nuclide migration calculations for a n-member chain. However, the maximum allowed time step is governed by the nuclide where the concentration changes are largest.

In practice, the modification added a number of DO-loops from 1 to ICHAIN, where ICHAIN is the number of members in the chain. The following subroutines were changed:

THERM, FINK, FLOW, SURE, SPECK, TALLY and DRT.

A number of variables were given an additional dimension to account for the members of the chain. These variables are given in Appendix 1. Specifically the following input variables have to be given for each nuclide: K_i (BLOCK 2) and λ_i (BLOCK 7) .

The algorithm was also changed to directly include the decay terms. The discretized form of the governing equation is:

$$K_\ell V_\ell \frac{\Delta c_\ell}{\Delta t} = \sum_b F_{\ell b}\, c_{\ell b} + \sum_m F_{\ell m}\, c_{\ell m} + \sum_b U_{\ell b}(c_b - c_\ell) + \sum_m U_{\ell m}(c_m - c_\ell) -$$

$$- K_\ell V_\ell \lambda\, c_\ell + K_\ell^{i-1} V_\ell \lambda^{i-1} c_\ell^{i-1} \qquad (1)$$

This equation may be written (Rasmuson et al., 1981) :

$$\Delta c_\ell = \Delta c_{\ell,exp} + \frac{\theta\Delta t}{K_\ell V_\ell}\left[\sum_m F_{\ell m}\Delta c_{up} - \sum_b U_{\ell b}\Delta c_\ell + \right.$$

$$\left. + \sum_m U_{\ell m}\,(\Delta c_m - \Delta c_\ell) - K_\ell V_\ell \lambda\, \Delta c_\ell\right] \qquad (2)$$

where:

$$\Delta c_{\ell,exp} = \frac{\Delta t}{K_\ell V_\ell}\left[\sum_b F_{\ell b} c_{\ell b} + \sum_m F_{\ell m}\left[\zeta c^o_{up} + (1-\zeta)c^o_{down}\right]\right.$$

$$+ \sum_b U_{\ell b}(c_b - c^o_\ell) + \sum_m U_{\ell m}(c^o_m - c^o_\ell) +$$

$$\left. + K_\ell^{i-1} V_\ell \lambda^{i-1} c_\ell^{i-1}\right] \qquad (3)$$

Rearranging equation (2), we get:

$$\left[1 + \frac{\theta\Delta t}{K_\ell V_\ell}\left[-\sum_{\substack{m\\ \ell=up}} F_{\ell m} + \sum_b U_{\ell b} + \sum_m U_{\ell m} + K_\ell V_\ell \lambda\right]\right]\Delta c_\ell$$

$$- \frac{\theta\Delta t}{K_\ell V_\ell}\left[\sum_{\substack{m\\ m=up}} F_{\ell m}\Delta c_{up} + \sum_m U_{\ell m}\,\Delta c_m\right] = \Delta c_{\ell,exp} \qquad (4)$$

These changes are accomodated by appropriate modifications of the TRUMP code.

The modification is done in HEART (Appendix 2). The decay constants λ_d are taken from SUBROUTINE SURE via COMMON/DECAY/LAMBDA (3). The variable I, denoting nuclide in chain, is transferred to SUBROUTINE SPECK via COMMON/CHAIN/I.

COMPARISON WITH ANALYTICAL SOLUTIONS

The migration of a chain of three radionuclides without matrix diffusion, is described by the following set of differential equations:

$$D_L \frac{\partial^2 c_1}{\partial z^2} - U_f \frac{\partial c_1}{\partial z} - R_1 \frac{\partial c_1}{\partial t} - R_1 \lambda_1 c_1 = 0 \tag{5}$$

$$D_L \frac{\partial^2 c_2}{\partial z^2} - U_f \frac{\partial c_2}{\partial z} - R_2 \frac{\partial c_2}{\partial t} - R_2 \lambda_2 c_2 + R_1 \lambda_1 c_1 = 0 \tag{6}$$

$$D_L \frac{\partial^2 c_3}{\partial z^2} - U_f \frac{\partial c_3}{\partial z} - R_3 \frac{\partial c_3}{\partial t} - R_3 \lambda_3 c_3 + R_2 \lambda_2 c_2 = 0 \tag{7}$$

Focusing on the equation for the second member, the first and second terms represent transport due to dispersion and convection. The third term represents accumulation, and the fourth and fifth terms represent disappearance of 2 by decay and appearance of 2 from decay of 1, respectively. R_i is the retardation factor and is defined by $R_i = 1 + K_i/\varepsilon_f$ where K_i is the volume equilibrium constant.

The boundary conditions at the inlet are given by the generalized Bateman equations (Bateman, 1910), which describe batch chain decay when all chain members have initial inventories.

$$c_1(o,t) = c_1^o \, e^{-\lambda_1 t} \tag{8}$$

$$c_2(o,t) = c_1^o \frac{\lambda_1}{\lambda_2 - \lambda_1} \left[e^{-\lambda_1 t} - e^{-\lambda_2 t} \right] + c_2^o \, e^{-\lambda_2 t} \tag{9}$$

$$c_3(o,t) = c_1^o \lambda_1\lambda_2\left[\frac{e^{-\lambda_1 t}}{(\lambda_2-\lambda_1)(\lambda_3-\lambda_1)} + \frac{e^{-\lambda_2 t}}{(\lambda_1-\lambda_2)(\lambda_3-\lambda_2)} + \right.$$

$$\left. + \frac{e^{-\lambda_3 t}}{(\lambda_1-\lambda_3)(\lambda_2-\lambda_3)}\right] + \qquad (10)$$

$$+ \frac{c_2^o \cdot \lambda_2}{\lambda_3-\lambda_2}\left[e^{-\lambda_2 t} - e^{-\lambda_3 t}\right] + c_3^o e^{-\lambda_3 t}$$

Using the Laplace transform technique, Lester et al. (1975) derived analytical solutions of the system (5)-(7), subject to the boundary conditions (8)-(10). The solution for the special case when $R_1 = R_2 = R_3$ and when nuclides 2 and 3 are not originally in the repository (i.e. $c_2^o = c_3^o = 0$), may be written in a simple form:

$$c_i(z,t) = c_i(o,t) \cdot c(z,t); \quad i=1,2,3 \qquad (11)$$

where:

$$c(z,t) = 0.5\left[\operatorname{erfc}(\text{arg } 1 - \text{arg } 2) + \right.$$

$$\left. + \exp(Pe)\operatorname{erfc}(\text{arg } 1 + \text{arg } 2)\right] \qquad (12)$$

$$\text{arg } 1 = \left(\frac{R\,Pe\,z}{4\,U_f t}\right)^{1/2}$$

$$\text{arg } 2 = \left(\frac{Pe\,U_f t}{4\,Rz}\right)^{1/2}$$

A computer program was written to evaluate (11) for different values of the parameters. In equation (11) the product of an exponential and the erfc must be taken. The erfc is always small while the exponential may be large. This difficulty is circumvented (for Pe > 100) by using the asymptotic expansion for erfc (x) (Abramowitz and Stegun, 1972 p. 298) :

$$\operatorname{erfc}(x) = \pi^{-\frac{1}{2}} x^{-1} e^{-x^2} \left[1 + \sum_{m=1}^{\infty} (-1)^m \frac{1 \cdot 3 \cdot \ldots \cdot (2m-1)}{(2x^2)^m} \right]$$

Computations made with the generalized TRUMP code (TRUCHN) were compared with the analytical solution (11). The parameter values used in the test problems, are given in Table 1. Figure 1 shows the case where $T_1 = 100$, $T_2 = 200$, and $T_3 = 300$ years. A very good agreement is obtained. This is also the case for $T_1 = 300$, $T_2 = 30$ and $T_3 = 3000$ years (Figure 2). For $T_1 = 100$, $T_2 = 1$ and $T_3 = 1000$ years, oscillations occur in the numerical solution for the second nuclide. This is of little importance, since for practical purposes the second membe: with $T_2 = 1$ may be deleted, and 3 may be assumed to form directly from 1. The errors incurred are small.

Parameter	Dimension	Value
U_f, Fluid Velocity	m/s	$1.0 \cdot 10^{-6}$
Pe, Peclet Number	-	0.5
R, Retardation Factor	m^3/m^3	$1.0 \cdot 10^3$
z, Distance from Source	m	$1.0 \cdot 10^2$
Δz, Length of Fracture Element	m	5 to 200

Table 1: Parameters used in the problems where $K_1 = K_2 = K_3$.

As a more complicated test case, we considered the three-member chain U - 238 → Th - 230 → Ra - 226 . The parameter values used for this case are given in Table 2. Note that $K_1 \neq K_2 \neq K_3$. The analytical solution for this case is complicated (Lester et al. 1975). The evaluation was done with the computer code GETOUT (Grundfelt, 1978). In the TRUMP calculation, different velocities must be given for each nuclide in the chain if sorption takes place at the fracture surfaces. To avoid this, the sorption was modelled as volume sorption in a thin slab (thickness α), adjacent to the fracture. The diffusivity was given a value such that, even at early times, the slab was essentially saturated. The relation between the surface and volume equilibrium constant is then $K_a = K\alpha$.

Figure 4 shows the good agreement which was obtained between the numerical and analytical solutions.

Parameter	Dimension	Value
U_f, Fluid Velocity	m/yr	5.684
$U_f b$, Fluid Flux	m^3/yr, breadth of fissure	$2.9841 \cdot 10^{-5}$
Pe, Peclet Number	-	0.5
S, Fracture Spacing	m	1.0
ε_f, Fracture Porosity	-	$1.05 \cdot 10^{-5}$
α, Thickness of Slab	m	$1.0 \cdot 10^{-4}$
K_i, Volume Equilibrium Constant	m^3/m^3	$(1.62; 1.35; 0.1701) \cdot 10^3$
$D_p \varepsilon_p$, Effective Diffusivity in Bulk Solid	m^2/yr	$4.5 \cdot 10^{-9}$ [a]
T_i, Half Life	yr	$4.51 \cdot 10^9$; $8 \cdot 10^4$; $1.6 \cdot 10^3$
2b, Fracture Aperture	m	$1.05 \cdot 10^{-5}$
K_p, Hydraulic Conductivity	m/s	10^{-9}
i, Hydraulic Gradient	m/m	0.002
z, Distance from Source	m	$2.25 \cdot 10^3$
Δz, Length of Fracture Element	m	50 - 1000 (12.5 - 1000)

a This value was chosen to saturate the slab in a reasonable time, and is not related to real matrix diffusivities.

Table 2: Parameters used in comparison with GETOUT

THE INFLUENCE OF MATRIX DIFFUSION

Examples

The effect of diffusion into the rock matrix on the migration of single radionuclides was investigated by Neretnieks (1980) and Rasmuson and Neretnieks (1981). The migration of the i^{th} member of a radionuclide chain, in a set of parallel fractures, is described by:

$$\frac{\partial c_f^i}{\partial t} + U_f \frac{\partial c_f^i}{\partial z} - D_L \frac{\partial^2 c_f^i}{\partial z^2} = - \frac{N^i}{b} - \lambda^i c_f^i + \lambda^{i-1} c_f^{i-1} \qquad (13)$$

$$K^i \frac{\partial c_p^i}{\partial t} = \varepsilon_p D_p \frac{\partial^2 c_p^i}{\partial x^2} - K^i \lambda^i c_p^i + K^{i-1} \lambda^{i-1} c_p^{i-1} \qquad (14)$$

and

$$N^i = - D_p \varepsilon_p \left(\frac{\partial c_p^i}{\partial x}\right)_{x=0} \qquad (15)$$

The first equation is the mass balance of the i^{th} member in the water in the fissures. The second equation is the mass balance in the rock matrix. Equation (15) is the coupling condition between (13) and (14).

To illustrate the impact of matrix diffusion on the arrival times of the members of a radionuclide chain, a number of numerical calculations were done for the two chains U-238 → Th-230 → Ra-226 and Pu-239 → U-235 → Pa-231. Data for the chain members are given in Tables 3 and 4.

Notice that there is a crucial difference between the two chains. The chain beginning with U-238 has a long-lived mother and a short-lived daughter, while the opposite is the case for the chain starting with Pu-239. This difference is of fundamental importance to the migration of the chain in the geological barrier.

	half life (years)	decay constant ($year^{-1}$)	volume equilibrium constant (m^3/m^3)
U-238	$4.51 \cdot 10^{9}$	$1.5369 \cdot 10^{-10}$	$1.62 \cdot 10^{3}$
Th-230	$8.0 \cdot 10^{4}$	$8.6643 \cdot 10^{-6}$	$1.35 \cdot 10^{3}$
Ra-226	$1.6 \cdot 10^{3}$	$4.3322 \cdot 10^{-4}$	$1.701 \cdot 10^{2}$

Table 3: Data for the decay chain
U-238 → Th-230 → Ra-226

	half life (years)	decay constant ($year^{-1}$)	volume equilibrium constant (m^3/m^3)
Pu-239	$2.44 \cdot 10^{4}$	$2.8408 \cdot 10^{-5}$	$1.08 \cdot 10^{2}$
U-235	$7.1 \cdot 10^{8}$	$9.7626 \cdot 10^{-10}$	$1.62 \cdot 10^{3}$
Pa-231	$3.25 \cdot 10^{4}$	$2.1328 \cdot 10^{-5}$	$1.944 \cdot 10^{3}$

Table 4: Data for the decay chain
Pu-239 → U-235 → Pa-231

The parameters used in the simulations are given in Table 5. Three different cases were investigated for each chain. The fracture aperture, porosity and fluid velocity were calculated from the model developed by Snow (1968) :

$$
\begin{aligned}
2b &= 0.0105\ (SK_p)^{1/3} \\
\varepsilon_f &= 2b/S \\
U_f \varepsilon_f &= K_p i
\end{aligned}
\qquad (16)
$$

The bed length parameter δ (given in Table 5) may be thought of as a ratio of one time, specifying the moving fluid, to another time, specifying the diffusion in particles. A low value of δ implies that only the outmost part of the rock is utilized for sorption, due to the short contact times. A high value of δ, on the other hand, is the case of long contact times, when the material behind the front reaches equilibrium (Rasmuson and Neretnieks, 1981). The range of δ used in the calculations exemplifies this.

Parameter		Case 1(2)	Case 3
K_p, Hydraulic Conductivity	m/s	10^{-9}	10^{-9}
i, Hydraulic Gradient	m/m	0.002	0.002
S, Fracture Spacing	m	1	50
2b, Fracture Aperture	m	$1.05 \cdot 10^{-5}$	$3.8682 \cdot 10^{-5}$
ε_f, Fracture Porosity		$1.05 \cdot 10^{-5}$	$7.7365 \cdot 10^{-7}$
U_f, Fluid Velocity	m/yr	5.684	81.4338
$U_f b$, Fluid Flux	$m^3/yr, m$	$2.9841 \cdot 10^{-5}$	$1.5750 \cdot 10^{-3}$
z, Distance from Source	m	22.5(2250)	325
t_w, Water Transport Time	yr	3.9585(395.85)	3.991
Pe, Peclet Number		0.5	0.5
D_L, Longitudinal Dispersion Coefficient	m^2/yr	$2.5578 \cdot 10^2(10^4)$	$5.2932 \cdot 10^4$
$D_p\varepsilon_p$, Effective Diffusivity in Bulk Solid	m^2/yr	$3.15 \cdot 10^{-5}$	$3.15 \cdot 10^{-5}$
δ, Bed Length Parameter (First Nuclide in Chain)		$1.5834 \cdot 10^1(10^3)$	$8.6665 \cdot 10^{-2}$

Table 5: Parameters used in examples.

To increase stability, the following device was used in the calculations. It was shown by Rasmuson and Neretnieks (1981) that for high values of K/m the breakthrough curve is practically independent of this parameter. This fact may be used to increase the stability of the calculations.

Large differences between the time constants of the volume elements mean slow convergence toward a solution. Accordingly, we wish to reduce these differences. We propose to increase the fracture aperture by a factor ω, thus increasing the time constants of the fracture elements, and reducing their relative differences. We divide U_f and D_L by ω, so terms $U_f b$ (the volume flow) and Pe (the Peclet number) are not affected. Finally, only the ratio K/m is changed, so our manipulation will have no effect on the breakthrough curve.

As in Rasmuson et.al (1981) we design the mesh in the rock matrix so that the mesh width increases by a factor β in the direction perpendicular to z.

Case 1: The results for the two chains are given in Figures 5 and 6. The fracture was divided into 13 volume elements, increasing in size from the inlet from 3 m (8) to 100 m (5). The matrix was divided into 15 volume elements in the direction perpendicular to z with 0.005 m (5) and then increasing in size by a factor $\beta = 1.4$. A factor $\omega = 10^3$ was used in the calculations.

In the figures, two additional sets of curves are given. These curves were computed with the computer program GETOUT. One set of curves gives results for surface sorption, while the other gives results for complete penetration of the rock matrix.

Notice that the differences in first arrival times are very large.

The time points corresponding to a concentration of 10^{-9} times that in the repository are given in Tables 6 and 7.

In the surface and volume sorption cases, the arrival times differ by as much as four orders of magnitude. The corresponding times for instationary diffusion are located between these extreme values. For the chain starting with Pu-239, these differences are especially pro-

nounced. Assuming surface sorption, Pu-239 arrives rapidly with a maximum relative concentration of $6.0 \cdot 10^{-1}$. For instationary diffusion, the time of first arrival is delayed by a factor of 10, and the maximum concentrati is only $5.4 \cdot 10^{-5}$. For volume sorption, the relative concentration is always less than 10^{-9}.

To investigate the sensitivity of the Pu-239 peak to variations in the equilibrium constant, a run was made with the K-values of Pu-239 and Pa-231 interchanged. The maximum concentration of Pu-239 now reaches $3 \cdot 10^{-8}$.

	Surface sorption	Instationary diffusion	Volume sorption
U-238	$8 \cdot 10^{2}$	$1 \cdot 10^{4}$	$4 \cdot 10^{6}$
Th-230	$4 \cdot 10^{4}$	$9 \cdot 10^{5}$	$9 \cdot 10^{6}$
Ra-226	$5 \cdot 10^{4}$	$2 \cdot 10^{6}$	$1 \cdot 10^{7}$

Table 6: Case 1, U-238 → Th-230 → Ra-226
Times for $c = 10^{-9}\ c_o$ on breakthrough curves.

	Surface sorption	Instationary diffusion	Volume sorption
Pu-239	$6 \cdot 10^{1}$	$7 \cdot 10^{2}$	-
U-135	$1 \cdot 10^{2}$	$6 \cdot 10^{3}$	$3 \cdot 10^{6}$
Pa-231	$< 1 \cdot 10^{4}$	$1 \cdot 10^{6}$	$8 \cdot 10^{6}$

Table 7: Case 1, Pu-239 → U-235 → Pa-231
Times for $c = 10^{-9}\ c_o$ on breakthrough curves.

Case 2: This case differs from case 1 only in that the distance from the source is one hundred times greater (2250 m). The fracture is treated a 37 discrete volume elements which increase in size from the inlet 50 m (10), to 100 m (20) and 1000 m (7). In this long contact time case, the rock matrix was treated as a single element (0.5 m). A stabilizing factor of $\omega = 10^{3}$ was used.

The results are shown in Figures 7 and 8, together with the surface sorption and complete volume sorption cases obtained with GETOUT. The arrival times of the 10^{-9} c_o concentrations are given in Tables 8 and 9. The curves for instationary diffusion and complete volume sorption now nearly coincide. This is due to the long contact times. For instationary diffusion and volume sorption, the relative concentration of Pu-239 is always less than 10^{-9}. This is not the case for surface sorption, where Pu-239 arrives with a maximum concentration of $1.5 \cdot 10^{-2}$.

	Surface sorption	Instationary diffusion	Volume sorption
U-238	$8 \cdot 10^4$	$2 \cdot 10^8$	$4 \cdot 10^8$
Th-230	$1 \cdot 10^5$	$8 \cdot 10^8$	$8 \cdot 10^8$
Ra-226	$2 \cdot 10^5$	$1 \cdot 10^9$	$1 \cdot 10^9$

Table 8: Case 2, U-238 → Th-230 → Ra-226
Times for $c = 10^{-9}$ c_o on breakthrough curves.

	Surface sorption	Instationary diffusion	Volume sorption
Pu-239	$6 \cdot 10^3$	-	-
U-235	$7 \cdot 10^3$	$2 \cdot 10^8$	$4 \cdot 10^8$
Pa-231	$< 1 \cdot 10^5$	$8 \cdot 10^8$	$9 \cdot 10^8$

Table 9: Case 2, Pu-239 → U-235 → Pa-231
Times for $c = 10^{-9}$ c_o on breakthrough curves.

Case 3: A fracture spacing of $S = 50$ m was used in this last example. The value of the bed length parameter is $\sim 10^{-1}$, implying that only the outer part of the rock matrix is penetrated. The mesh was in the fracture 50 m (8) and 500 m (5), and in the matrix 13 elements increasing in size with a factor $\beta = 1.8$ with initial element 0.005 m and a large last element. ω was again given the value 10^3.

The resulting curves are given in Figures 9 and 10.

Matrix diffusion decoupled from flowing water

To investigate the impact of the rock matrix on the radionuclide chain migration, diffusion (and sorption) in a porous medium was studied separately. Two different two-member chains were studied:

	U-238	→ Th-230
half life (years)	$4.51 \cdot 10^9$	$8.0 \cdot 10^4$

and:

	Pu-239	→ U-235
half life (years)	$2.44 \cdot 10^4$	$7.1 \cdot 10^8$

The fundamental difference in these chains lies in the ratio of the half-life of the first nuclide to that of the second. For each chain member two values of the volume equilibrium constant K, were used: K = 1 and $K = 10^4$. Accordingly, we get four combinations of K-sets: 1, 1; 1, 10^4; 10^4, 1; 10^4, 10^4.

Analytical solution

For a two-member chain with $U_f = 0$ (only diffusion):

$$D \frac{\partial^2 c_1}{\partial z^2} - K_1 \frac{\partial c_1}{\partial t} - K_1 \lambda_1 c_1 = 0 \qquad (17)$$

$$D \frac{\partial^2 c_2}{\partial z^2} - K_2 \frac{\partial c_2}{\partial t} - K_2 \lambda_2 c_2 + K_1 \lambda_1 c_1 = 0 \qquad (18)$$

The analytical solution of this system, for a semi-infinite medium, may be obtained from Lester et al. (1975) by taking the limit as $U_f \to 0$.

For the special case when $K_1 = K_2$ and nuclide 2 is not originally in the repository, we have:

$$\lim_{U_f \to 0} Pe = 0$$

$$\lim_{U_f \to 0} \arg 1 = z/2\sqrt{\frac{D}{K}t}$$

$$\lim_{U_f \to 0} \arg 2 = 0$$

Thus:

$$c_i(z,t) = c_i(o,t)\ c(z,t); \quad i = 1,2 \tag{19}$$

where:

$$c(z,t) = \operatorname{erfc}\left(\frac{z}{2\sqrt{\frac{D}{K}t}}\right) \tag{20}$$

$$c_1(o,t) = c_1^o\ e^{-\lambda_1 t} \tag{21}$$

$$c_2(o,t) = c_2^o \frac{\lambda_1}{\lambda_2 - \lambda_1}\left[e^{-\lambda_1 t} - e^{-\lambda_2 t}\right] \tag{22}$$

For a decaying band release we obtain:

$$c'(z,t) = c(z,t) - c(z,t-T)\ H(t-T) \tag{23}$$

where H is Heaviside's step function and T is the leach time.

From here on, for the sake of simplicity, we omit the prime in c'.

Using (23), we may now calculate the molar flux at the surface:

$$N_i = - D \left.\frac{\partial c_i}{\partial z}\right|_{z=0} \qquad [\mathrm{mol/m^2,s}] \tag{24}$$

We have :

$$\frac{\partial c_i}{\partial z} = c_i(o,t)\left[- \frac{2}{\sqrt{\pi}} \exp\left(- \frac{z^2}{4\frac{D}{K}t} \right) \frac{1}{2\sqrt{\frac{D}{K}t}} + \right.$$

$$\left. + \frac{2}{\sqrt{\pi}} \exp\left(- \frac{z^2}{4\frac{D}{K}(t-T)} \right) \frac{1}{2\sqrt{\frac{D}{K}(t-T)}} H(t-T) \right] \tag{25}$$

For $z = 0$ we get :

$$\left.\frac{\partial c_i}{\partial z}\right|_{z=0} = c_i(0,t)\left[- \frac{1}{\sqrt{\pi \frac{D}{K} t}} + \frac{1}{\sqrt{\pi \frac{D}{K}(t-T)}} H(t-T) \right] \tag{26}$$

Finally we obtain N_i as:

$$N_i = c_i(o,t) \sqrt{\frac{DK}{\pi}} \left[\frac{1}{\sqrt{t}} - \frac{1}{\sqrt{t-T}} H(t-T) \right] \tag{27}$$

Note that N_i is positive for $t \leq T$ (transport into the porous material) and negative for $t > T$ (transport out).

The mass in the matrix per unit area of the fracture at time t is obtained by integrating eq. 23 with respect to z (and multiplying by K):

$$M_z = K \int_o^\infty c_i(o,t) \left[\operatorname{erfc} \frac{z}{2\sqrt{\frac{D}{K}t}} - \operatorname{erfc} \frac{z}{2\sqrt{\frac{D}{K}(t-T)}} H(t-T) \right] dz$$

$$= c_i(o,t)\, 2\sqrt{\frac{DK}{\pi}} \left[\sqrt{t} - \sqrt{t-T}\, H(t-T) \right] [\mathrm{mol/m^2}] \tag{28}$$

On the other hand, the integration of N_i with respect to time gives the amount M_t that has been transported across the outer surface.

To obtain M_t we must evaluate the integrals:

$$\int_0^t e^{-\lambda t}\, t^{-\frac{1}{2}}\, dt = \sqrt{\frac{\pi}{\lambda}}\, \mathrm{erf}\, \sqrt{\lambda t} \qquad (29)$$

[Gradshteyn and Ryzhik, 1965, 3.361]

and:

$$\int_T^t e^{-\lambda t}(t-T)^{-\frac{1}{2}} dt = \left| \begin{array}{c} u = t - T \\ du = dt \\ (T,t) \rightarrow (0,\ t-T) \end{array} \right| =$$

$$= \int_0^{t-T} e^{-\lambda(u+T)}\, u^{-\frac{1}{2}} du = e^{-\lambda T} \sqrt{\frac{\pi}{\lambda}}\, \mathrm{erf}\, \sqrt{\lambda(t-T)} \qquad (30)$$

For the first nuclide (i=1), we get:

$$M_t = \int_0^t N_1\, dt = c_1^o \sqrt{\frac{DK}{\lambda_1}} \left[\mathrm{erf}\, \sqrt{\lambda_1 t} - e^{-\lambda_1 T}\, \mathrm{erf}\, \sqrt{\lambda_1 (t-T)} \cdot H(t-T) \right] \qquad (31)$$

$[\mathrm{mol/m^2}]$

At the end of the leach period ($t = T$), we have :

$$M_T = \int_0^T N_1\, dt = c_1^o \sqrt{\frac{DK}{\lambda_1}}\, \mathrm{erf}\, \sqrt{\lambda_1 T} \qquad (32)$$

For $t > T$, the amount that has been transported out of the system (across the plane $z = 0$) is given by $M_T - M_t$.

It is interesting to note that for $t \leq T$, $M_z \leq M_t$. This is due to the fact that the nuclide decays with time. For a non-decaying species, $M_z = M_t$.

Similarly, for the second member of the chain (i = 2) we obtain:

$$M_t = \int_o^t N_2 dt = c_1^o \frac{\lambda_1\sqrt{DK}}{\lambda_2 - \lambda_1}\left[\frac{1}{\sqrt{\lambda_1}}\left[\operatorname{erf}\sqrt{\lambda_1 t} - e^{-\lambda_1 T}\operatorname{erf}\sqrt{\lambda_1 (t-T)}\cdot H(t-T)\right] - \frac{1}{\sqrt{\lambda_2}}\left[\operatorname{erf}\sqrt{\lambda_2 t} - e^{-\lambda_2 T}\operatorname{erf}\sqrt{\lambda_2 (t-T)}\cdot H(t-T)\right]\right] \quad (33)$$

For $t = T$ we obtain:

$$M_T = \int_o^T N_2\, dt = \frac{\lambda_1\sqrt{DK}}{\lambda_2 - \lambda_1}\left[\frac{1}{\sqrt{\lambda_1}}\operatorname{erf}\sqrt{\lambda_1 T} - \frac{1}{\sqrt{\lambda_2}}\operatorname{erf}\sqrt{\lambda_2 T}\right] \quad (34)$$

The amount that has been transported out of the system ($t > T$) is again given by $M_T - M_t$.

For $t > T$, and introducing $a = t/T$, equation (27) may be written as:

$$N_i = c_i(o,t)\sqrt{\frac{DK}{\pi T}}\left[\frac{1}{\sqrt{a}} - \frac{1}{\sqrt{a-1}}\right] = c_i(o, aT)\, g(K,T)\, f(a) \quad (35)$$

where:

$$g(K,T) = \sqrt{\frac{DK}{\pi T}} \quad (36)$$

D=const.

$$f(a) = \frac{1}{\sqrt{a}} - \frac{1}{\sqrt{a-1}} \left(\approx -\frac{1}{2a\sqrt{a}}\right), \quad a \gg 1 \quad (37)$$

and $c_i(o, aT)$ are given by equations (21) and (22).

The surface concentrations $c_i(o, aT)$ for the two chains are shown in Figures 11 and 12 as a function of a for two values of T, $3 \cdot 10^4$ and $5 \cdot 10^5$ years. Note that $c_i(o,aT)$ is nearly constant for the chain U-238 → → Th-230, but that this is not the case for the chain Pu-239 → U-235.

Note that what is actually shown is the inventory of the nuclides in a closed system. The time scale t/T is used in order to facilitate the use of equation 35.

The entity g(K,T) as a function of K for the two values of T is shown in Figure 13. The diffusivity D is treated as a constant with the value $3.15 \cdot 10^{-5}$ m^2/yr. In the same figure, the function -f(a) is also shown. -f(a) decreases rapidly with $a (\sim 0.5\ a^{-3/2})$.

Thus, the molar flux N_i is obtained by taking the product of $c_i(o,aT)$ which is dependent of both nuclide and time, g(K,T) which depends on equilibrium constant and leach time, and f(a) which depends on t/T only.

A computer program DIFCHA was written to evaluate the analytical solution. Input data are the equilibrium constant K, the diffusivity D, the half-lives T_1 and T_2, and the leach time TLEAK. Outputs are values for boundary concentration, flux and integrated flux for the two nuclides.

When $K_1 \neq K_2$, the analytical solution for the second nuclide is much more complicated. For these cases it was decided to use the numerical code instead. However, the analytical solution is given here for reference. The solution for $U_f = 0$ may again be obtained by limiting procedures. Since a number of errors were found in the solution given by Lester et al. (1975), the corresponding solution given by Burkholder and Rosinger (1979) was used. The solution is given in Appendix 3, together with the redefined functions F. The limiting values of F and $\partial F/\partial z$ as $z \to 0$ are also given (they are needed for the calculation of the flux at the surface). Since the expressions within the square-root signs may become negative, complex arithmetic must be used. Since the complex parts cancel, the total expression is real (as it should be).

We have, for example

$$F_{20}^{-}(1,2)F_{25}^{-}(2,1) + F_{20}^{+}(1,2)F_{25}^{+}(2,1) =$$

$$= F_{20}^{-}F_{25}^{-} + \overline{F_{20}^{-}F_{25}^{-}} = 2\,\mathrm{Re}\{F_{20}^{-}F_{25}^{-}\}$$

Numerical solution

The following cases, for the two chains U-238 → Th-230 and Pu-239 → U-235 were calculated with the computer program TRUCHN:

leach time $T = 3 \cdot 10^4$ years

fissure spacing S = 50 m

and the four combinations of K-values $(1,1),(1,10^4)$, $(10^4,1)$, $(10^4,10^4)$.

The matrix was divided into 41 volume elements with the first element length of 0.01 m. The lengths then increase by a factor of 1.16 (last element 1.3924 m). In one case, however, (Pu-239 → and $K_1 = K_2 = 10^4$), a finer mesh was used (first element has a length of 0.001 m and then increases by a factor 1.24, last element 2.2712 m).

The molar flux at the surface is shown in Figures 14-17 for the U-238 chain and in Figures 18-21 for the Pu-239 chain. The analytical solution equation (27), where $K = K_1$, is also given for reference. Note that the absolute value of N_i is shown; for $t > T$, N_i is negative.

In Figures 14-15 and 18-19, the numerical solutions (for $K_1 = K_2$ may be compared with the analytical solution (equation (27)). The agreement is very good except for the second nuclide when $K = 1$ (the value of N_2 is very low). Here, oscillations occurred, especially when $t < T$. However, the behaviour of N_2 immediately after the contact period was predicted accurately. The solution may be improved by taking shorter time steps. Note, that according to equation (27) N_i is proportional to $\sqrt{K}$. Thus, the curves for $K = 10^4$ are obtained by multiplying the N_i values for $K = 1$ by 100.

In Figures 16-17 and 20-21, the numerical solutions are shown for K_1 not equal to K_2. For $K_1 = 1$ and $K_2 = 10^4$ (Figure 16), the flux of Th-230 (in the U-238 chain) is initially higher for $t > T$ than the reference. However, after the initial period, N_2 decreases rapidly compared to the reference case At first (for $t > T$), there is a high concentration of Th-230 in a thin layer close to the fracture. This causes the beginning period of high flux. After the depletion of this layer, the subsequent generation from U-238 is highly immobile, and the flux decreases rapidly.

For $K_1 = 10^4$ and $K_2 = 1$ (Figure 17), the Th-230 outflow after $t > T$ is always higher than the reference. The low value of K_2 makes Th-230 very mobile.

For the Pu-239 chain the situation is somewhat different. For $K_1 = 1$ and $K_2 = 10^4$ (Figure 20), the outflow of U-235 is higher than in the reference case. Due to its short half-life Pu-239, is rapidly converted into U-235, and does not have time to move very far into the matrix. Thus, U-235, is concentrated in a rock layer adjacent to the surface. For $K_1 = 10^4$ and $K_2 = 1$ (Figure 21) the situation is interesting because there is outflow of U-235 when $t < T$. This is due to the combination of the short half-life of Pu-239 and the low K-value of U-235 (in comparison to that of Pu-239). In a thin surface layer a high concentration of U-235 builds up. As a consequence of this outflow, the matrix is depleted of U-235, and the flux for $t > T$ is comparatively low.

Ratio of daughter to parent nuclide activity outflows

The reconcentration effect

Sometimes it is difficult to apply numerical methods to calculations about the migration of a nuclide decay chain. To ease these difficulties, we wish to describe the outflow of a daughter nuclide in terms of the outflow of its parent nuclide.

Note that it is incorrect to assume secular equilibrium in the outflow from an aquifer in which the different nuclides in the decay chain move with different velocities (Burkholder and Cloninger 1976).

The factor by which the activity outflow of a nuclide exceeds the activity outflow of its parent nuclide is called the reconcentration factor.

We may express the reconcentration factor RCF as

$$RCF = \frac{\phi_d \lambda_d}{\phi_p \lambda_p} \tag{38}$$

where ϕ is the molar flux (mole, s^{-1}, m^{-2})

λ is the decay constant (s^{-1})

and the indices d and p stand for the daughter nuclide and its parent nuclide, respectively.

Under certain circumstances, the RCF takes on a limiting value of R_p/R_d ,

where R is the retardation factor defined by

$$U_i = \frac{U_f}{R_i} \tag{39}$$

where U_f is the water flow velocity in the aquifer (m/s)

U_i is the velocity of the nuclide i (m/s)

A more complete discussion may be found in Appendix 4. Only the basic structure is shown below.

In order for the derivation to be strictly valid, the following conditions must be met:

a) A daughter nuclide must decay much faster than its parent nuclide.

b) A daghter nuclide must move much faster than its parent nuclide.

c) The aquifer must be long enough to allow any original input of the daughter nuclide to decay completely.

The outflow of a radionuclide at a time T is composed of contributions from radioactive decay of its parent nuclide further upstream at $t \leq T$. We may calculate the activity outflow of the daughter nuclide from the distribution of its parent nuclide at $t = T$ if we disregard the effect of dispersion between the time the contribution took place and the outflow. However, we are interested only in the ratio between the two nuclides, so the effect of the dispersion may be expected to cancel out to some extent.

The ratio of activity outflows may be written as

$$\frac{\phi_d \lambda_d}{\phi_p \lambda_p} = \frac{R_p}{R_d} \left(1 - e^{-\frac{L \cdot R_d \lambda_d}{U_f}} \cdot \left(1 - \frac{R_d}{R_p} e^{\frac{L \cdot R_d \lambda_p}{U_f}} \right) \right) \qquad (40)$$

where L is the length of the aquifer. Note that, as the length of the aquifer increases, the ratio of activity outflows will go from 1 to R_p/R_d.

Comparison of the retarding effects of instationary diffusion into rock matrix versus surface - and volume sorption

The retardation factors are calculated as

$$R = 1 + K \cdot \alpha \left(\frac{1 - \varepsilon_f}{\varepsilon_f} \right) \qquad (41)$$

for the surface- and volume- sorption cases where, ε_f is given by (16).

We see that R is roughly proportional to K with the same constant of proportionality for the different nuclides in one case.

The different K-values are as shown in Tables 3 and 4. These K-values are the same for all the studied cases, even the ones including stationary diffusion.

When instationary diffusion into the rock matrix takes place, we can no longer define a retardation factor for the system as a whole, since the penetration depth is no longer constant.

The decay pairs of interest are U-238 to Th-230, Th-230 to Ra-226 and (in spite of a higher velocity for the parent nuclide) U-235 to Pa-231.

The ratio of the activity releases of a nuclide to that of its parent nuclide at a fixed time are shown in Figures 22 to 27. For comparison, the ratio of the K values of the parent nuclide to its daughter nuclide are shown.

Table 10. Daughter- to Parent Activity Outflows Ratio Around Maximum Outflow. xx)

Nuclide	Case x)	Surface sorption	Matrix diffusion	Volume sorption
U238-Th230	1	1.1 (1.1)	1.1	1.1 (1.1)
	2	1.2 (1.2)	1.2	1.2 (1.2)
	3	0.95(1.0)	1.1	-
Th230-Ra226	1	6.0 (7.9)	7.0	7.9 (7.9)
	2	7.9 (7.9)	7.9	7.9 (7.9)
	3	4.5 (6.4)	-	-
U235-Pa231	1	0.5 (0.8)	0.7	0.8 (0.8)
	2	0.8 (0.8)	0.8	0.8 (0.8)

x) The cases are numbered as in Table 5

xx) The values inside parenthesises are calculated by means of equation (40) and (41)

Table 10 shows activity outflow ratios in which a stable value has been attained. This value varies by less than a factor of 2 while the release of the daughter nuclide is greater than 10^{-5} times its maximum value, except for those parts of the curves where numerical problems like instability cause erroneous results. Those parts of the curves that suffer most from numerical instability have been removed for the sake of legibility.

Conclusions

The theoretical model derived above gives a qualitatively correct picture in the cases studied here, within the limitations imposed by the derivation of eq. (40).

It is surprising that, although instationary diffusion into the rock matrix considerably changes the general appearance of the release curves, it hardly affects the ratio of the daughter to parent nuclide releases. However, in all cases studied, the distribution coefficients of the daughter- and parent nuclides differ by less than a factor of 10. This means that the penetration depths of the nuclides in the decay chains are relatively

similar. Therefore the results cannot be used to formulate any general criterion as to when chain decay may be omitted from migration calculations. Figures 16 and 17 show that the ratio of the daughter- and parent nuclide fluxes at the rock/crack interface varies considerably with time when the differences in distribution coefficients become large. Thus it is difficult to apply the results of this study to other parameter values.

NOTATION

a	$= t/T$	
b	half width of fissure	m
c	concentration	mol/m^3
c^o	initial concentration of mother nuclide or concentration at beginning of time step	mol/m^3
c_f	concentration in liquid in fissures	mol/m^3
$c_{\ell b}$	concentration at the boundary surface segment of node ℓ	mol/m^3
$c_{\ell m}$	concentration at the interface between volume elements ℓ and m	mol/m^3
c_ℓ	concentration in node ℓ	mol/m^3
c_m	concentration in node m	mol/m^3
c_p	concentration in liquid in microfissures	mol/m^3
Δc	difference in concentration	mol/m^3
D_L	longitudinal dispersion coefficient	m^2/s
$D_p \varepsilon_p$	effective diffusivity in bulk solid (sometimes denoted by D only)	m^2/s
$F_{\ell b}$	volumetric fluid flux between the boundary and node ℓ	m^3/s
$F_{\ell m}$	volumetric fluid flux between nodes ℓ and m	m^3/s
i	hydraulic gradient	m/m
K	volume equilibrium constant	m^3/m^3
K_a	surface equilibrium constant	m^3/m^2
K_ℓ	volume equilibrium constant of element ℓ	m^3/m^3
K_p	hydraulic conductivity	m/s
L	length of aquifer	m
M_z	mass in rock matrix at time t, per unit fracture surface	mol/m^2
M_t	mass transported across fracture-solid interface, per unit fracture surface	mol/m^2

m	$= \frac{\varepsilon_f}{1-\varepsilon_f}$	
N	molar flux at the fracture-solid interface	$mol/m^2,s$
Pe	$= zU_f/D_L$, Peclet number	
R	retardation factor	
S	fissure spacing	m
t	time	s
Δt	time step	s
T	leach time	s
T_i	half life	s
U_f	water velocity	m/s
$U_{\ell b}$	conductance at the boundary surface segment of volume element ℓ	m^3/s
$U_{\ell m}$	conductance between nodes ℓ and m	m^3/s
V_ℓ	volume of element ℓ	m^3
x	distance into rock matrix	m
z	distance in flow direction	m
Δz	length of fracture element	m

Greek letters

α	penetration thickness	m
β	mesh spacing factor	
δ	$\frac{1.33\ D_p\ \varepsilon_p}{S^2} \cdot \frac{z}{mU_f}$, bed length parameter	
ε_f	fracture porosity	m^3/m^3

ζ	upstream weighting factor	
θ	implicit weighting factor for the time domains	
λ	decay constant of radionuclide	s^{-1}
ϕ	flux of dissolved species	mol/m^2, s
ω	factor to increase stability in numerical solution	

Subscript or superscript

i	i^{th} chain member

Subscript

p	parent nuclide
d	daughter nuclide

REFERENCES

Abramovitz, M. and I.A. Stegun, Handbook of Mathematical Functions. Dover, New York,1972.

Bateman, H., Proc. Cambridge Phil. Soc. 15, 423 (1910).

Burkholder, H.C. and M.O. Cloninger: The reconcentration phenomenon of radionuclide chain migration BNWL-SA-5786 (1976).

Burkholder, H.C. and E.L.J. Rosinger: A model for the transport of radionuclides and their decay products through geologic media. Atomic Energy of Canada Limited, AECL-6325 (1979).

Edwards, A.L., TRUMP: A computer program for transient and steady state temperature distributions in multidimensional systems, National Technical Information Service, National Bureau of Standards, Springfield Va. 1969.

Gradshteyn, I.S. and I.M. Ryzhik: Tables of Integrals, Series, and Products. Academic Press 1965.

Grundfelt, B.: Nuklidvandring från ett bergförvar för utbränt bränsle (Swedish). KBS TR 77 (1978).

Lester, D.H., G. Jansen and H.C. Burkholder: Migration of radionuclide chains through an adsorbing medium. AIChE Symposium Series No. 152 — Adsorption and Ion Exchange, 71, 202 (1975).

Narasimhan, T.N. and P.A. Witherspoon: An integrated finite difference method for analyzing fluid flow in porous media. Water Resources Res. 12, 57 (1976).

Neretnieks, I.: Diffusion in the rock matrix: An important factor in radionuclide retardation ? J. Geophys. Res. 85, 4379 (1980).

Rasmuson, A. and I. Neretnieks: Migration of radionuclides in fissured rock: The influence of micropore diffusion and longitudinal dispersion. J. Geophys. Res. 86, 3749 (1981).

Rasmuson, A., T.N. Narasimhan and I. Neretnieks: Chemical transport in a fissured rock: Verification of a numerical model. Water Resources Res. Accepted for publication (1981).

Snow, D.T.: Rock fracture spacings, openings and porosities. J. Soil Mech. Found. Div., Amer. Soc. Civil Eng. 94 (SM1) 73 (1968).

APPENDIX 1: Variables modified in TRUMP

The variables given below (already existing in the TRUMP code) where all given an additional dimension I to account for the radionuclide chain members.

N = number of nodes

I = length of chain

THERM

CAPT(12,10,I)	capacity K:

SURE

FB(20,I)	total mass added to system from boundary node NODB(N)
FS(20,I)	total mass flow from NODSB(N) to NODS(N) at SUMTIM
TB(20,I)	concentration at boundary node NODB(N)
TBS(20,I)	average value of TB(N,I) in a time step
TIMEB(12,20,I)	decay constant λ_i

TALLY

DTEMP(I)	maximum concentration change in a time step DELTS (last time step completed)
RAST(I)	
RAT1(I)	value of TVARY/DTEMP in time step DELTS
RAT2(I)	value of TVARY/DTEMP in time step DELTSS (last accepted time step completed before DELTS)
RATG(I)	value of TVARY/DTEMP in time step DELTG (last accepted time step completed)
SLOPS(I)	ratio of maximum rates of concentration change in time steps DELTS and DELTSS, (RAT1 * DELTS)/ (RAT2 * DELTSS)

COMMON BLOCKS

BLANK COMMON

CAP(N,I)	capacity of NODE(N); $\rho K_i V$
DDT(N,I)	estimated rate of change of T(N,I) (c_i) in next time step
DF(N,I)	net mass flow into NODE(N) in time step DELT
DFI(N,I)	mass flow from NOD2(N) to NOD1(N) in time step DELT
DT(N,I)	change in concentration in NODE(N) in time step DELT
FI(N,I)	total mass flow from NOD2(N) to NOD1(N) at SUMTIM
ICHAIN	number of nuclides in chain
SLIM(N,I)	maximum stable time step for a regular NODE(N), equals CAP(N,I)/ ZIP(N,I)
T(N,I)	concentration in NODE(N)
TRAN(N,I)	conductance between NOD1(N) and NOD2(N)
W(N,I)	mass in NODE(N)
ZIP(N,I)	overall conductance for NODE(N)

COMMON/ASURES/ (SURE, SPECK)

DFS(20,I)	mass flow from NODSB(N) to NODS(N) in time step DELT
TRANS(20,I)	conductance between NODS(N) and NODSB(N)

COMMON/AA/(TALLY)

F(N,I)	total mass flow into NODE(N) at SUMTIM
H(N,I)	mass added to NODE(N) up to SUMTIM

COMMON/DECAY/(HEART, SURE)

LAMBDA(I)	decay constant λ_i

COMMON/CHAIN/(HEART, SPECK)

I	calculation for i^{th} chain member

APPENDIX 2: Modification of TRUMP code

The modification is done at the end of the main program (HEART).

```
4205 CALL THERM                                                          HEART.2
     IF(NOGEN  .NE. Ø) CALL GEN                                          HEART.2
     IF(NOCON  .NE. Ø) CALL FINK                                         HEART.2
     IF(NOFLOW .NE. Ø) CALL FLOW                                         HEART.2
     IF(NOSCON .NE. Ø) CALL SURE                                         HEART.2
     IF(NMELT  .NE. Ø) CALL THERM1                                       HEART.2
     DO 9Ø1Ø I=1,ICHAIN
     DO 44Ø6 N=1,NODES
     ZIP(N,I)=ZIP(N,I)+LAMBDA(I)*CAP(N,I)
     IF(I.GT.1)GOTO 44Ø7
     DT(N,I)=DT(N,I)-LAMBDA(I)*T(N,I)*DELT
     GOTO 44Ø6
44Ø7 DT(N,I)=DT(N,I)-LAMBDA(I)*T(N,I)*DELT+
    1(CAP(N,I-1)/CAP(N,I))*LAMBDA(I-1)*(T(N,I-1)-(1.-FOR)*
    2DT(N,I-1))*DELT
4406 CONTINUE
     IF(NOSPEC .NE. Ø) CALL SPECK                                        HEART.29
9Ø1Ø CONTINUE
```

APPENDIX 3: Limiting form ($U_f \to 0$) of an analytical solution (with dispersion) given by Burkholder and Rosinger (1979).

$$C_{1,d} = \frac{1}{2} F_1(1) \left[F_{13}(1) \left(F_{23}^-(1) - F_{24}^-(1)\right) + F_{19}(1) \left(F_{23}^+(1) - F_{24}^+(1)\right)\right]$$

$$C_{2,d} = \frac{1}{2} F_2(2,1) \left[F_{13}(2) \left(F_{23}^-(2) - F_{24}^-(2)\right) + F_{19}(2) \left(F_{23}^+(2) - F_{24}^+(2)\right)\right]$$

$$+ \frac{1}{2} F_3(1,2) \left[F_{13}(1) \left(F_{23}^-(1) - F_{24}^-(1)\right) + F_{19}(1) \left(F_{23}^+(1) - F_{24}^+(1)\right)\right]$$

$$+ \frac{1}{2} F_4(1,2) \left[F_{20}^-(1,2) \left(F_{25}^-(2,1) - F_{26}^-(2,1)\right) + F_{20}^+(1,2) \left(F_{25}^+(2,1) - F_{26}^+(2,1)\right)\right]$$

$$+ \frac{1}{2} F_3(1,2) \left[F_{21}^-(1,2) \left(F_{27}^-(1,2,2,1) - F_{27}^-(1,2,1,2)\right) + F_{21}^+(1,2) \left(F_{27}^+(1,2,2,1) - F_{27}^+(1,2,1,2)\right)\right]$$

$$- \frac{1}{2} F_3(1,2) \left[F_{22}^-(1,2,1) \left(F_{28}^-(1,2,2,1) - F_{28}^-(1,2,1,2)\right) + F_{22}^+(1,2,1) \left(F_{28}^+(1,2,2,1) - F_{28}^+(1,2,1,2)\right)\right]$$

The functions F for $U_f \to 0$

$$F_1(i) = c_i^o$$

$$F_2(i,j) = c_i^o + c_j^o \left(\frac{\lambda_j}{\lambda_j - \lambda_i} \right)$$

$$F_3(i,j) = c_i^o \left(\frac{\lambda_i}{\lambda_j - \lambda_i} \right) \frac{K_i}{K_j}$$

$$F_4(i,j) = c_i^o \left(\frac{\lambda_i}{\lambda_j - \lambda_i} \right) \left(1 - \frac{K_i}{K_j} \right)$$

$$F_{13}(i) = \exp(-\lambda_i t)$$

$$F_{19}(i) = F_{13}(i)$$

$$F_{20}(i,j) = \exp \left[-\lambda_i t \pm z \sqrt{\frac{K_j(\lambda_j - \lambda_i)}{D}} \right]$$

$$F_{21}(i,j) = \exp \left[-\frac{K_i \lambda_i - K_j \lambda_j}{K_i - K_j} t \pm z \sqrt{\frac{K_i K_j (\lambda_j - \lambda_i)}{D(K_i - K_j)}} \right]$$

$$F_{22}(i,j,k) = \exp \left[-\frac{K_i \lambda_i - K_j \lambda_j}{K_i - K_j} t \pm z \sqrt{\frac{K_i K_j (\lambda_j - \lambda_i)}{D(K_i - K_j)}} - \left(\lambda_k - \frac{K_i \lambda_i - K_j \lambda_j}{K_i - K_j} \right) T \right]$$

$$F_{23}(i) = \operatorname{erfc} \left(\frac{z}{2} \sqrt{\frac{K_i}{Dt}} \right)$$

$$F_{24}(i) = H(t - T) \operatorname{erfc} \left(\frac{z}{2} \sqrt{\frac{K_i}{D(t-T)}} \right)$$

$$F_{25}(i,j) = \text{erfc}\left(\frac{z}{2}\sqrt{\frac{K_i}{Dt}} \pm \sqrt{(\lambda_i - \lambda_j)\,t}\right)$$

$$F_{26}(i,j) = H(t-T)\,\text{erfc}\left(\frac{z}{2}\sqrt{\frac{K_i}{D(t-T)}} \pm \sqrt{(\lambda_i - \lambda_j)(t-T)}\right)$$

$$F_{27}(i,j,k,\ell) = \text{erfc}\left(\frac{z}{2}\sqrt{\frac{K_k}{Dt}} \pm \sqrt{\frac{K_\ell(\lambda_j - \lambda_i)}{K_i - K_j}\,t}\right)$$

$$F_{28}(i,j,k,\ell) = H(t-T)\,\text{erfc}\left(\frac{z}{2}\sqrt{\frac{K_k}{D(t-T)}} \pm \sqrt{\frac{K_\ell(\lambda_j - \lambda_i)}{K_i - K_j}\,(t-T)}\right)$$

Values of $F_{20} - F_{28}$ at $z = 0$

$$F_{20}(i,j) = \exp(-\lambda_i t)$$

$$F_{21}(i,j) = \exp\left(-\frac{K_i\lambda_i - K_j\lambda_j}{K_i - K_j}\, t\right)$$

$$F_{22}(i,j,k) = \exp\left(-\frac{K_i\lambda_i - K_j\lambda_j}{K_i - K_j}\, t - \left(\lambda_k - \frac{K_i\lambda_i - K_j\lambda_j}{K_i - K_j}\right)T\right)$$

$$F_{23}(i) = 1$$

$$F_{24}(i) = H(t - T)$$

$$F_{25}(i,j) = \operatorname{erfc}\left(\pm\sqrt{(\lambda_i - \lambda_j)\, t}\right)$$

$$F_{26}(i,j) = H(t - T)\, \operatorname{erfc}\left(\pm\sqrt{(\lambda_i - \lambda_j)(t - T)}\right)$$

$$F_{27}(i,j,k,\ell) = \operatorname{erfc}\left(\pm\sqrt{\frac{K_\ell(\lambda_j - \lambda_i)}{K_i - K_j}\, t}\right)$$

$$F_{28}(i,j,k,\ell) = H(t - T)\, \operatorname{erfc}\left(\pm\sqrt{\frac{K_\ell(\lambda_j - \lambda_i)}{K_i - K_j}\,(t - T)}\right)$$

Values of $\frac{\partial F_{20}}{\partial z} - \frac{\partial F_{28}}{\partial z}$ at $z = 0$

$$F'_{20}(i,j) = \pm \sqrt{\frac{K_j(\lambda_j - \lambda_i)}{D}} \exp(-\lambda_i t)$$

$$F'_{21}(i,j) = \pm \sqrt{\frac{K_i K_j(\lambda_j - \lambda_i)}{D(K_i - K_j)}} \exp\left(-\frac{K_i\lambda_i - K_j\lambda_j}{K_i - K_j} t\right)$$

$$F'_{22}(i,j,k) = \pm \sqrt{\frac{K_i K_j(\lambda_j - \lambda_i)}{D(K_i - K_j)}} \exp\left(-\frac{K_i\lambda_i - K_j\lambda_j}{K_i - K_j} t - \left(\lambda_k - \frac{K_i\lambda_i - K_j\lambda_j}{K_i - K_j}\right) T\right)$$

$$F'_{23}(i) = -\sqrt{\frac{K_i}{\pi D t}}$$

$$F'_{24}(i) = -H(t - T)\sqrt{\frac{K_i}{\pi D(t - T)}}$$

$$F'_{25}(i,j) = -\sqrt{\frac{K_i}{\pi D t}} \exp\left[-(\lambda_i - \lambda_j) t\right]$$

$$F'_{26}(i,j) = -H(t - T)\sqrt{\frac{K_i}{\pi D(t - T)}} \exp\left[-(\lambda_i - \lambda_j)(t - T)\right]$$

$$F'_{27}(i,j,k,\ell) = -\sqrt{\frac{K_k}{\pi D t}} \exp\left[-\frac{K_\ell(\lambda_j - \lambda_i)}{K_i - K_j} t\right]$$

$$F'_{28}(i,j,k,\ell) = -H(t - T)\sqrt{\frac{K_k}{\pi D(t - T)}} \exp\left[-\frac{K_\ell(\lambda_j - \lambda_i)}{K_i - K_j} (t - T)\right]$$

APPENDIX 4

A simple analytical model for the migration of a nuclear decay chain

Here we describe the migration of a nuclear decay chain when the different components move with different velocities.

Consider a volume element with length Δz moving along the z-axis with the velocity of a daughter nuclide

$$U_d = U_f/R_d \qquad 1$$

If the concentration of its parent nuclide at the element's current position is C_p (molecules/m^3), we obtain a production of daughter nuclide:

$$\Delta z \cdot A \cdot C_p \cdot R_p (s^{-1}) \qquad 2$$

where A is the cross-sectional area of the aquifer (m^2).

Consider the situation in which a daughter nuclide moves faster than its parent nuclide. We may now regard the quantity of daughter nuclide in the studied volume element as the sum of contributions from decay of its parent nuclide further upstream at an earlier time, minus the decay those contributions have undergone in the time t that has elapsed since their formation.

If we define a z-axis parallel to U_f (but running in the opposite direction) with zero at the outlet we can show how far the two nuclides have moved at time t, when the daughter nuclide reaches the outlet, as in Fig 1:

Fig. 1 Relative positions of daughter- and parent nuclide

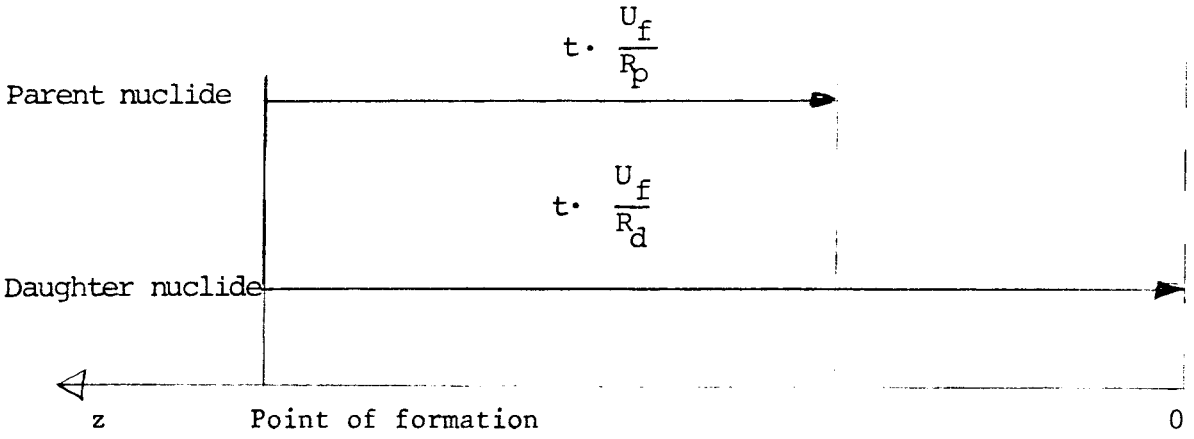

From Figure 1, we see that the location of the parent nuclide at time t may be written as:

$$z = t \left(\frac{U_f}{R_d} - \frac{U_f}{R_p}\right) \qquad 3$$

or, solving for t,

$$t = \frac{z}{U_f\left(\frac{1}{R_d} - \frac{1}{R_p}\right)} \qquad 4$$

Suppose that we know the concentration of parent nuclide as a function of z at some given time, and wish to calculate the release of daughter nuclide at this time, assuming no dispersion other than that which has already occurred in the parent distribution data for the element z.

The net contribution of daughter nuclide at the outlet may be written as

$$\Delta z \cdot A \cdot C_p(z) \cdot \lambda_p \cdot e^{\frac{z \cdot \lambda_p}{U_d - U_p}} \cdot e^{-\frac{z \cdot \lambda_d}{U_d - U_p}} \quad (s^{-1}) \qquad 5$$

Since $dt = \frac{1}{U_d - U_p} dz$, integration yields

$$C_d = \frac{\lambda_p}{U_d - U_p} \int_0^{L(1-\frac{R_d}{R_p})} C_p(z) e^{-z\cdot\frac{(\lambda_d - \lambda_p)}{U_d - U_p}} dz \qquad 6$$

Where L is (so far) an arbitrary constant length (m).
This leaves us with

$$\phi_d = \frac{\lambda_p}{R_d(U_d - U_p)} \int_0^{L(1-\frac{R_d}{R_p})} C_p(z) e^{-z\cdot\frac{(\lambda_d - \lambda_p)}{U_d - U_p}} dz \qquad 7$$

Since the outflow of parent nuclide may be written as:

$$\phi_p = \frac{C_p(0) U_f}{R_p} \qquad 8$$

We may write the ratio of outflows (in activity units) as:

$$\frac{\lambda_d \phi_d}{\lambda_p \phi_p} = \frac{\lambda_d}{C_p(0) R_d} \quad \frac{R_p}{(U_d - U_p)} \int_0^{L(1-\frac{R_d}{R_p})} C_p(z)\, e^{-z\cdot\frac{(\lambda_d - \lambda_p)}{U_d - U_p}} dz \qquad 9$$

Since we assume that no dispersion occurs, we may set

$$C_p(z) e^{z\frac{\lambda_p}{(U_d - U_p)}} = \text{constant} = C_p(0) \qquad 10$$

Equation 9 and 10 give

$$\frac{\lambda_d \phi_d}{\lambda_p \phi_p} = \frac{R_p}{R_d} \left(1 - e^{-L\cdot\frac{\lambda_d R_d}{U_f}}\right) \qquad 11$$

Eq (11) shows that, if the length of the aquifer substantially exceeds $\lambda_d R_d/U_f$, then the ratio of activity outflows will approach R_p/R_d.

Consider the situation when the aquifer is shorter. Now we have a contribution from the inflow of daughter nuclide activity in addition to the incomplete buildup of activity in the aquifer. Assume an inflow in secular equilibrium, i.e., we input equal activity flows of daughter and parent nuclide.

Let us begin with an inflow of 1 Ci/s for each parent- and daughter nuclide at a time t_{start}. By the time the daughter nuclide flow reaches the end of the aquifer t_{end}, it will have decayed to $e^{-\frac{L \cdot R_d}{U_f} \lambda_d}$.

The parent nuclide flow which reaches the outlet at t_{end} started at $t = t_{start}$ from a point $(1-\frac{R_d}{R_p})\,L$ from the beginning of the aquifer.

This parent nuclide flow was

$$e^{\frac{(1-\frac{R_d}{R_d})R_p \cdot \lambda_p \cdot L}{U_f}}$$ Ci at its inflow

and since it decays by a factor $e^{-\frac{L \cdot R_p \cdot \lambda_p}{U_f}}$ during

the passage through the aquifer, we have a daughter- to parent activity outflow ratio

$$= \frac{e^{-\frac{R_d \lambda_d}{U_f} L}}{e^{\frac{(1-\frac{R_d}{R_p})R_p \lambda_p L}{U_f}} e^{-\frac{L \cdot R_p \lambda_p}{U_f}}} = e^{-\frac{L \cdot R_d (\lambda_d - \lambda_p)}{U_f}} \qquad 12$$

If we add this contribution to the outflow given by (11) we get:

$$\frac{\lambda_d \, \phi_d}{\lambda_p \, \phi_p} = \frac{R_p}{R_d} \left(1 - e^{-\frac{L \cdot R_d \, \lambda_d}{U_f} \left(1 - \frac{R_d}{R_p} \, e^{\frac{L \cdot R_d \, \lambda_p}{U_f}} \right)} \right) \qquad 13$$

FIGURE CAPTIONS

Figure 1: Comparison with analytical solution $K_1 = K_2 = K_3$. Data given in Table 1. The half lives are $T_1 = 100$, $T_2 = 200$ and $T_3 = 300$ years.

Figure 2: Same as Figure 1 for $T_1 = 300$, $T_2 = 30$ and $T_3 = 3000$ years.

Figure 3: Same as Figure 1 for $T_1 = 100$, $T_2 = 1$ and $T_3 = 1000$ years.

Figure 4: Comparison with analytical solution evaluated by GETOUT for the chain U-238 → Th-230 → Ra-226. Data given in Table 2. $K_1 \neq K_2 \neq K_3$.

Figure 5: The influence of matrix diffusion as compared to surface and volume sorption (GETOUT).
Case 1, U-238 → Th-230 → Ra-226.
Data given in Tables 3-5.

Figure 6: Same as Figure 5 for Case 1, Pu-239 → U-235 → Pa-231.

Figure 7: Same as Figure 5 for Case 2, U-238 → Th-230 → Ra-226.

Figure 8: Same as Figure 5 for Case 2, Pu-239 → U-235 → Pa-231.

Figure 9: The influence of matrix diffusion at short contact times. Calculation with TRUCHN. Case 3, U-238 → Th-230 → Ra-226. Data given in Tables 3-5.

Figure 10: Same as Figure 9 for Case 3, Pu-239 → U-235 → Pa-231.

Figure 11: Boundary concentrations $c_i(0, aT)$ for the chain U-238 → Th-230 for two values of T; $3 \cdot 10^4$ and $5 \cdot 10^5$ years.

Figure 12: Boundary concentrations $c_i(0, aT)$ for the chain Pu-239 → U-235 for two values of T; $3 \cdot 10^4$ and $5 \cdot 10^5$ years.

Figure 13: The function $g(K, T)$ for two values of T; $3 \cdot 10^4$ and $5 \cdot 10^5$ years. In same diagram $-f(a)$.

Figure 14: Flux at the surface for U-238 → Th-230 and $K_1 = K_2 = 1$. Analytical solution (DIFCHA) and numerical solution (TRUCHN). For $t > T$ N is negative i.e. the nuclide is transported out of the matrix.

Figure 15: Same as Figure 14 for U-238 → Th-230 and $K_1 = K_2 = 10^4$.

Figure 16: Flux at the surface for U-238 → Th-230 and $K_1 = 1$, $K_2 = 10^4$. Analytical solution for $K_1 = K_2 = 1$ given as reference.

Figure 17: Flux at the surface for U-238 → Th-230 and $K_1 = 10^4$, $K_2 = 1$. Analytical solution for $K_1 = K_2 = 10^4$ given as reference.

Figure 18: Same as Figure 14 for Pu-239 → U-235 and $K_1 = K_2 = 1$.

Figure 19: Same as Figure 14 for Pu-239 → U-235 and $K_1 = K_2 = 10^4$.

Figure 20: Flux at the surface for Pu-239 → U-235 and $K_1 = 1$, $K_2 = 10^4$. Analytical solution for $K_1 = K_2 = 1$ given as reference.

Figure 21: Flux at the surface for Pu-239 → U-235 and $K_1 = 10^4$, $K_2 = 1$. Analytical solution for $K_1 = K_2 = 10^4$ given as reference.

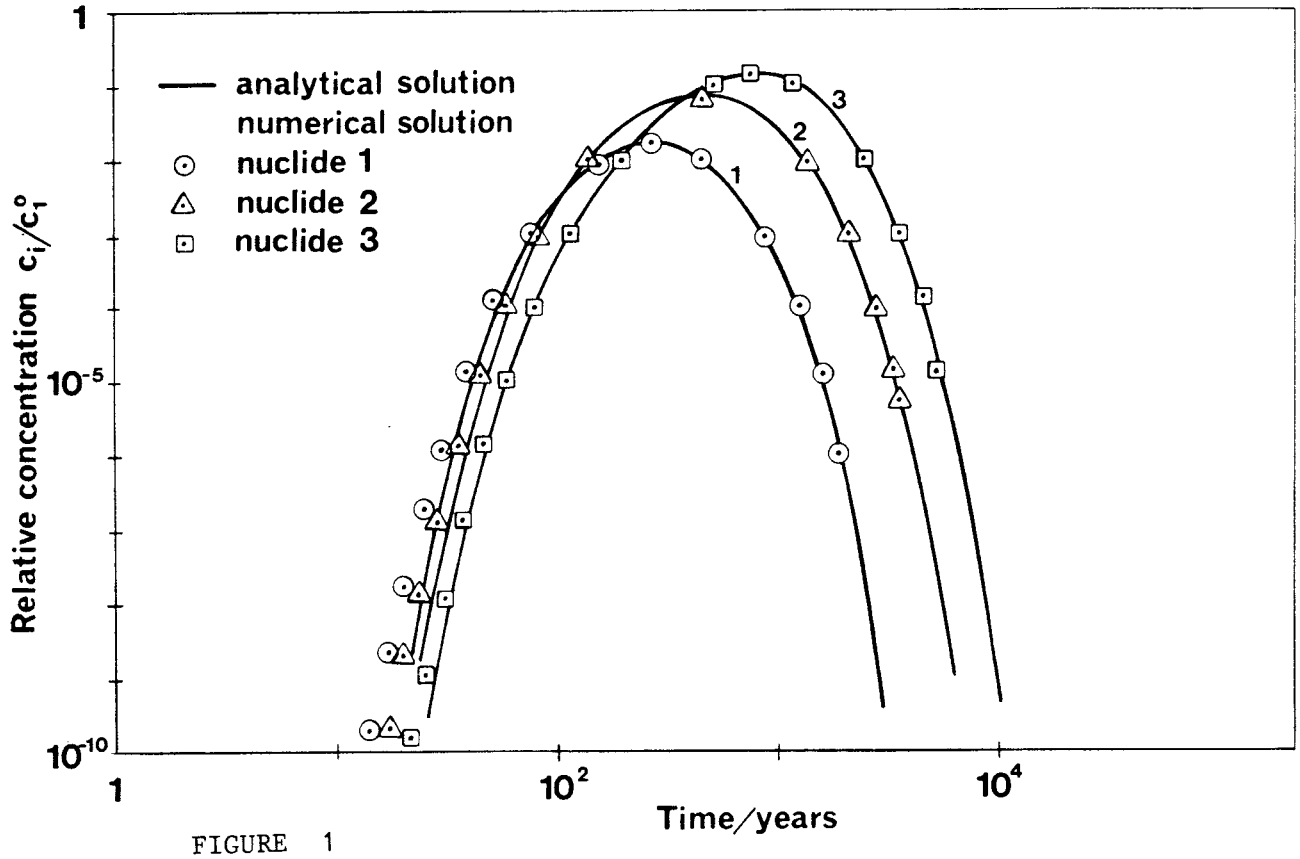

FIGURE 1

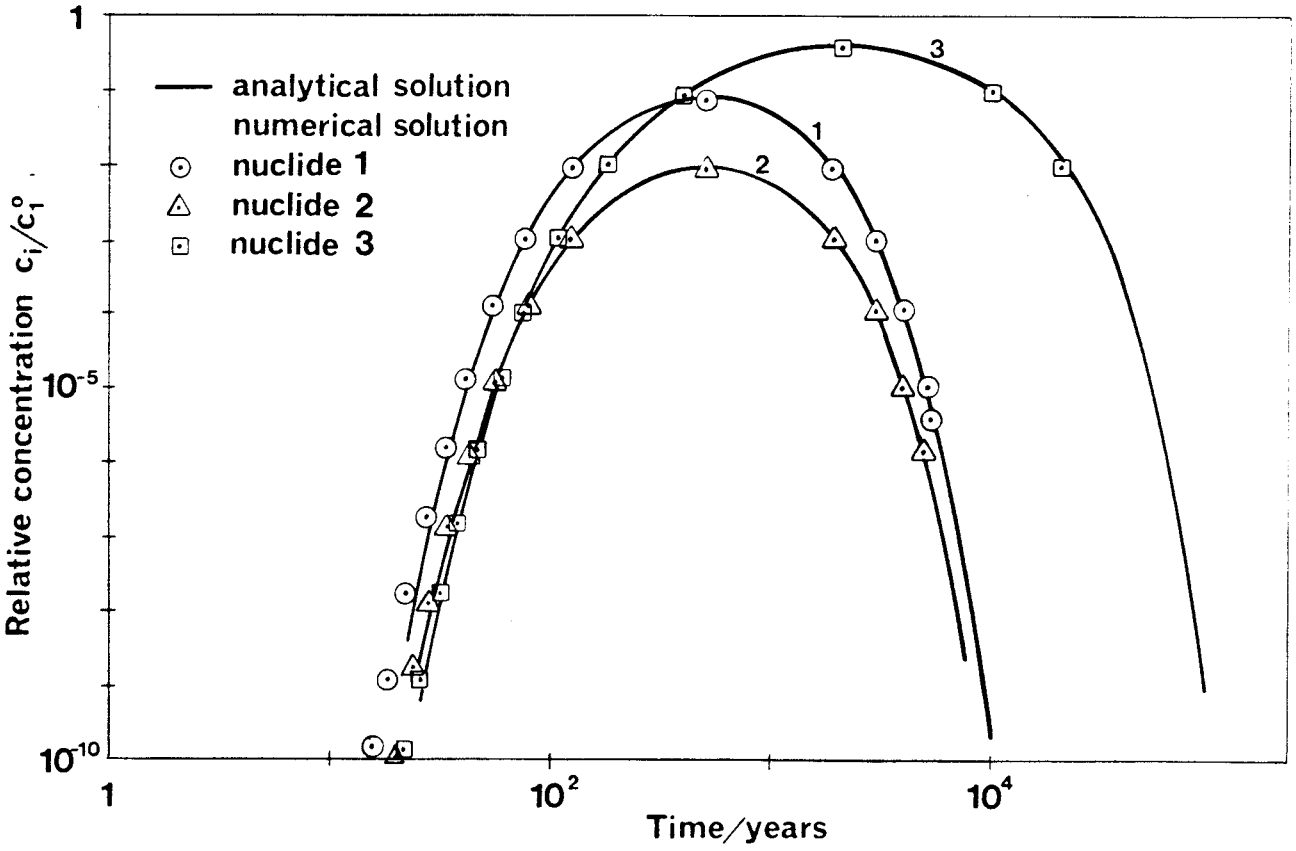

FIGURE 2

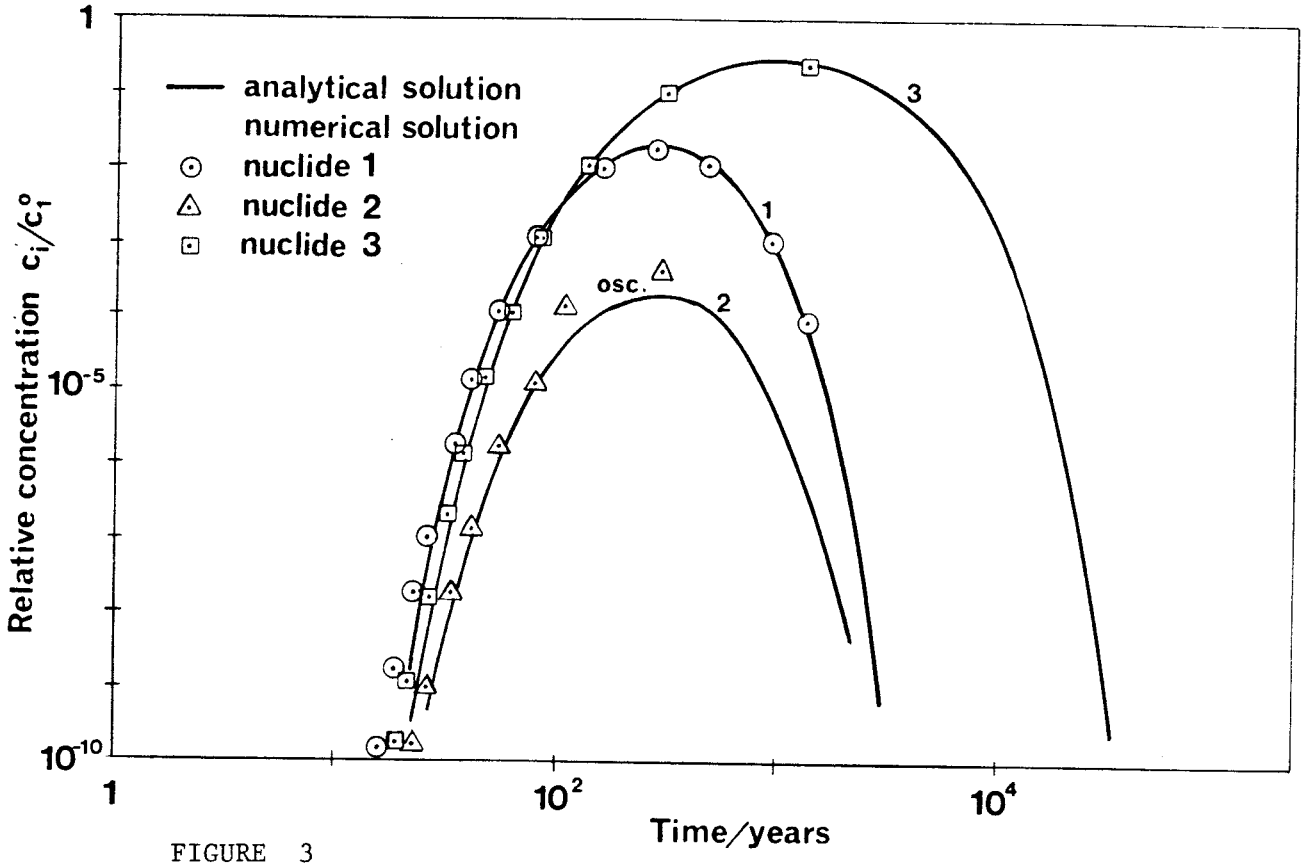

FIGURE 3

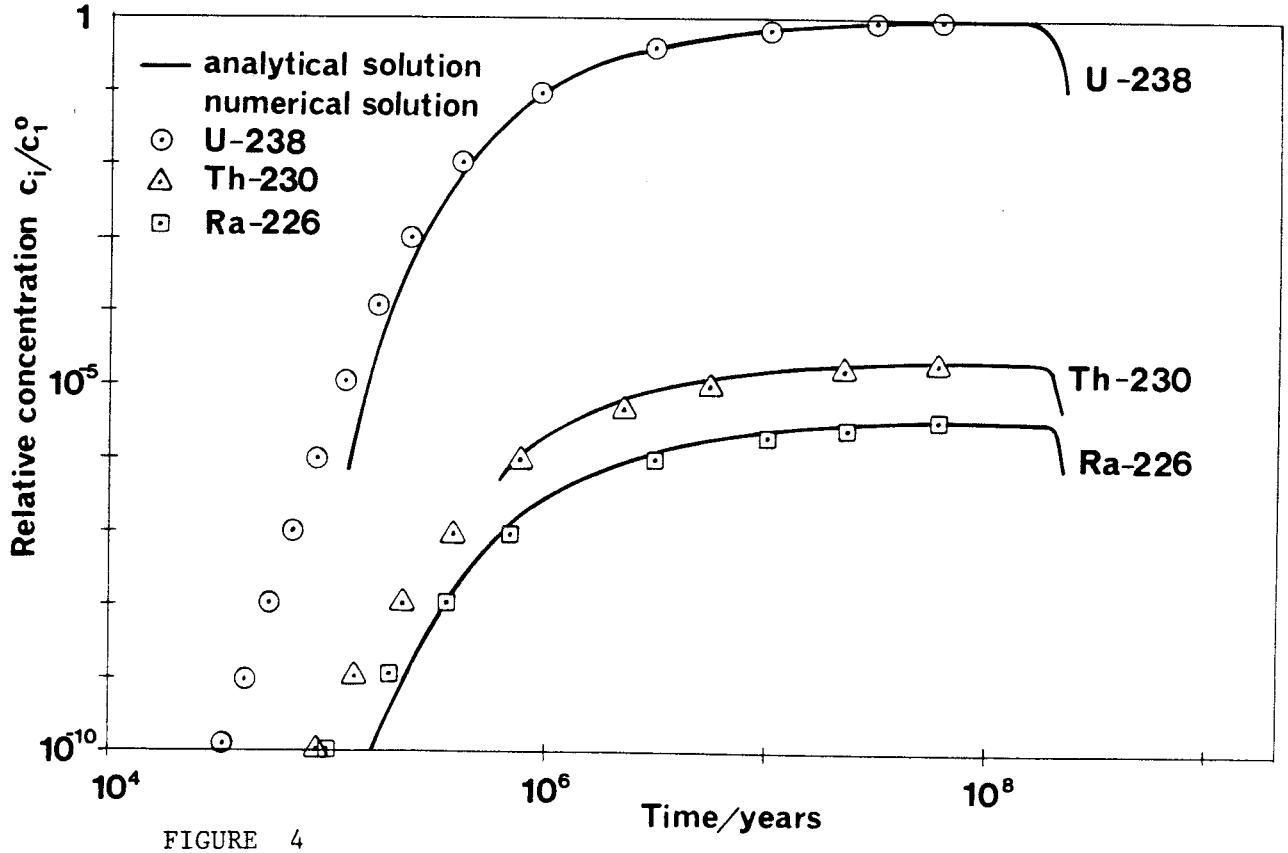

FIGURE 4

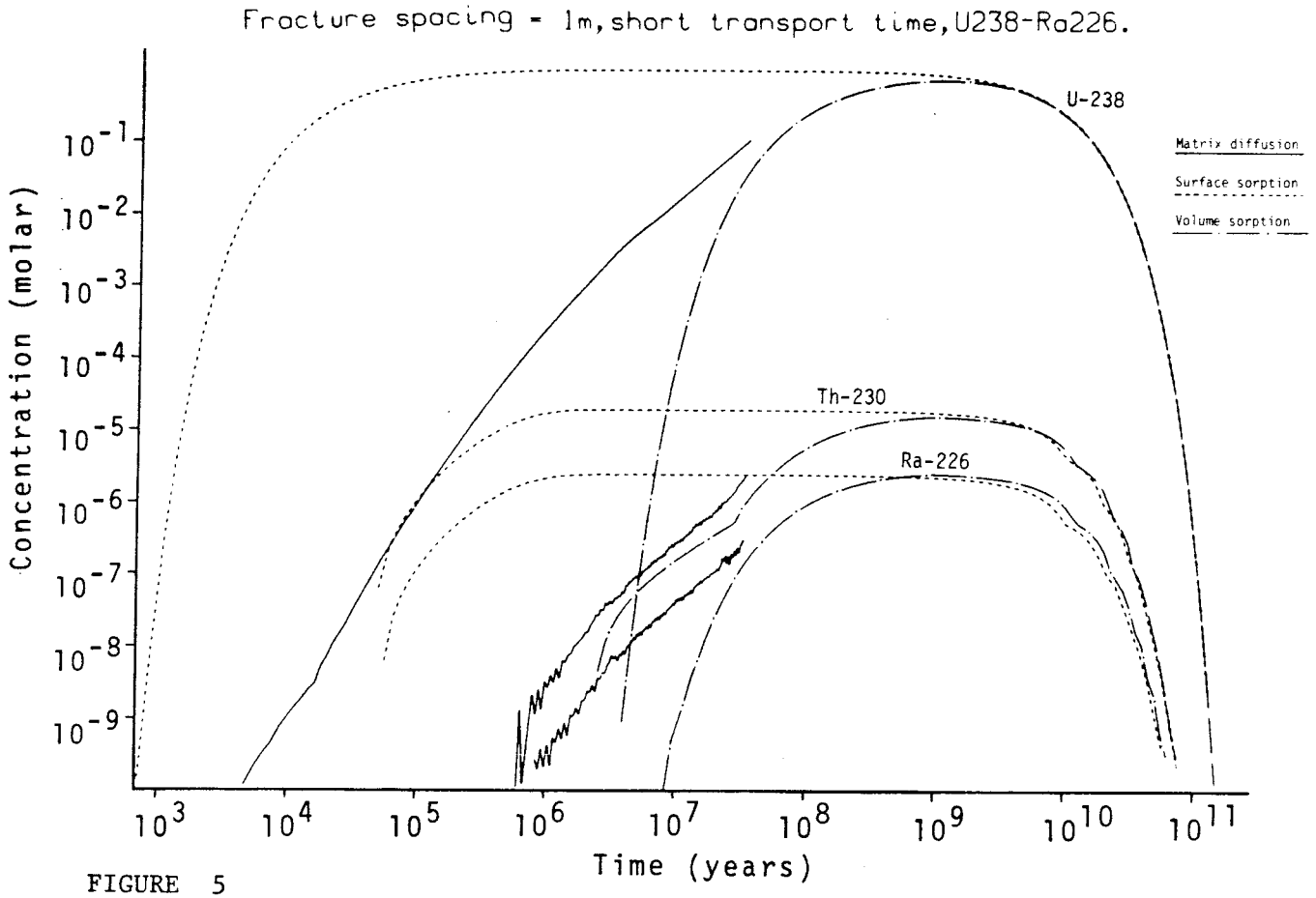

FIGURE 5

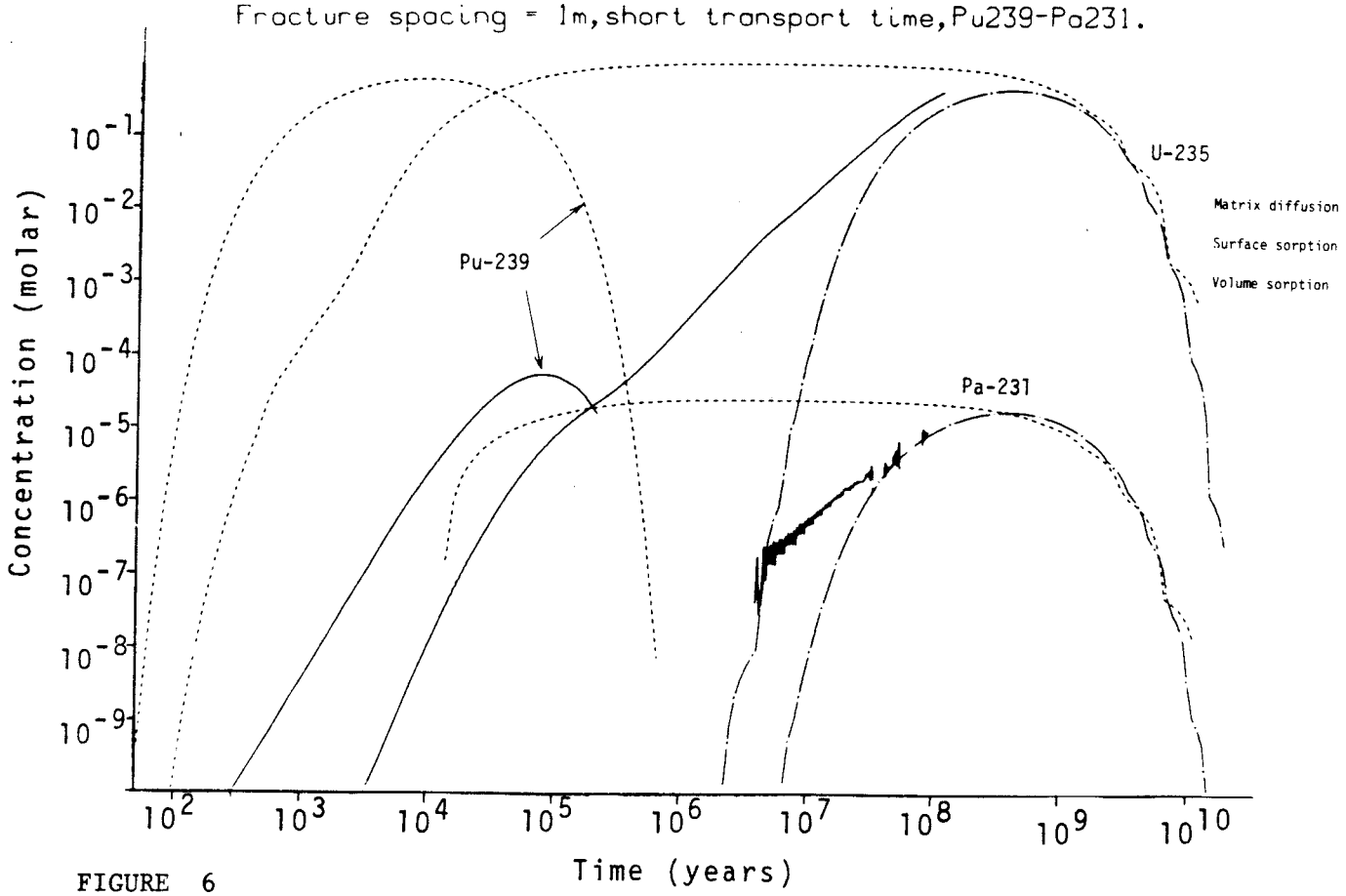

FIGURE 6

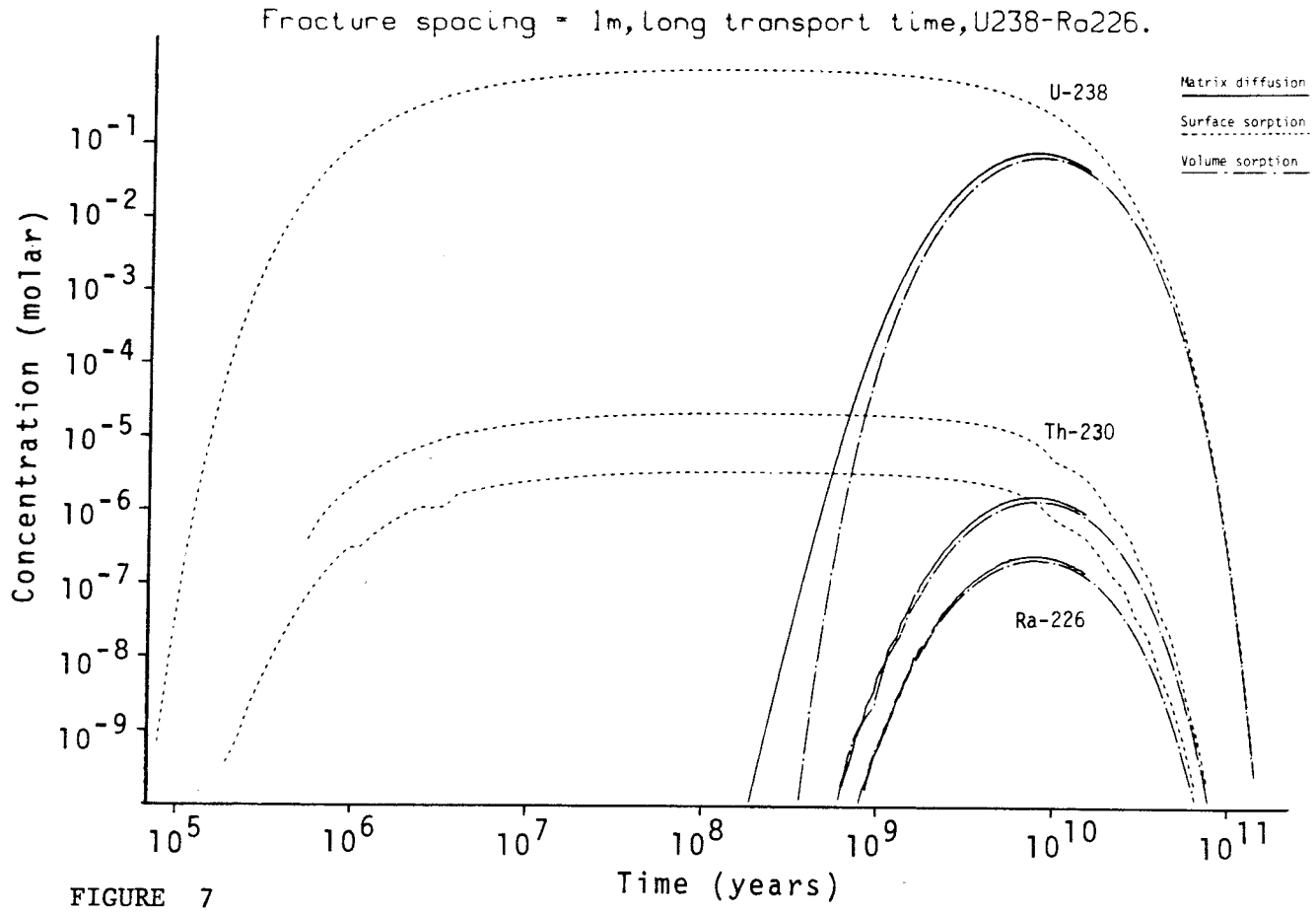

FIGURE 7

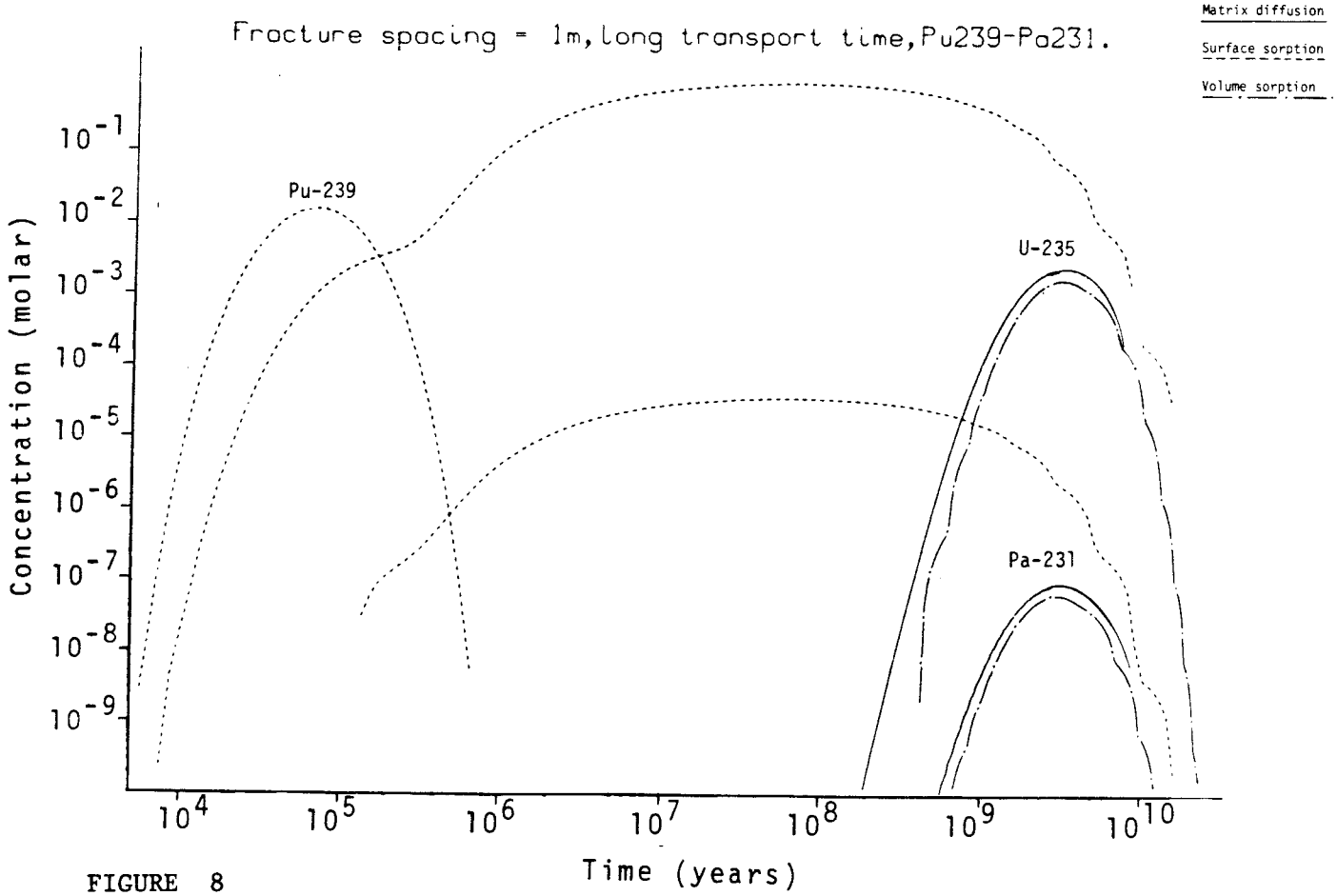

FIGURE 8

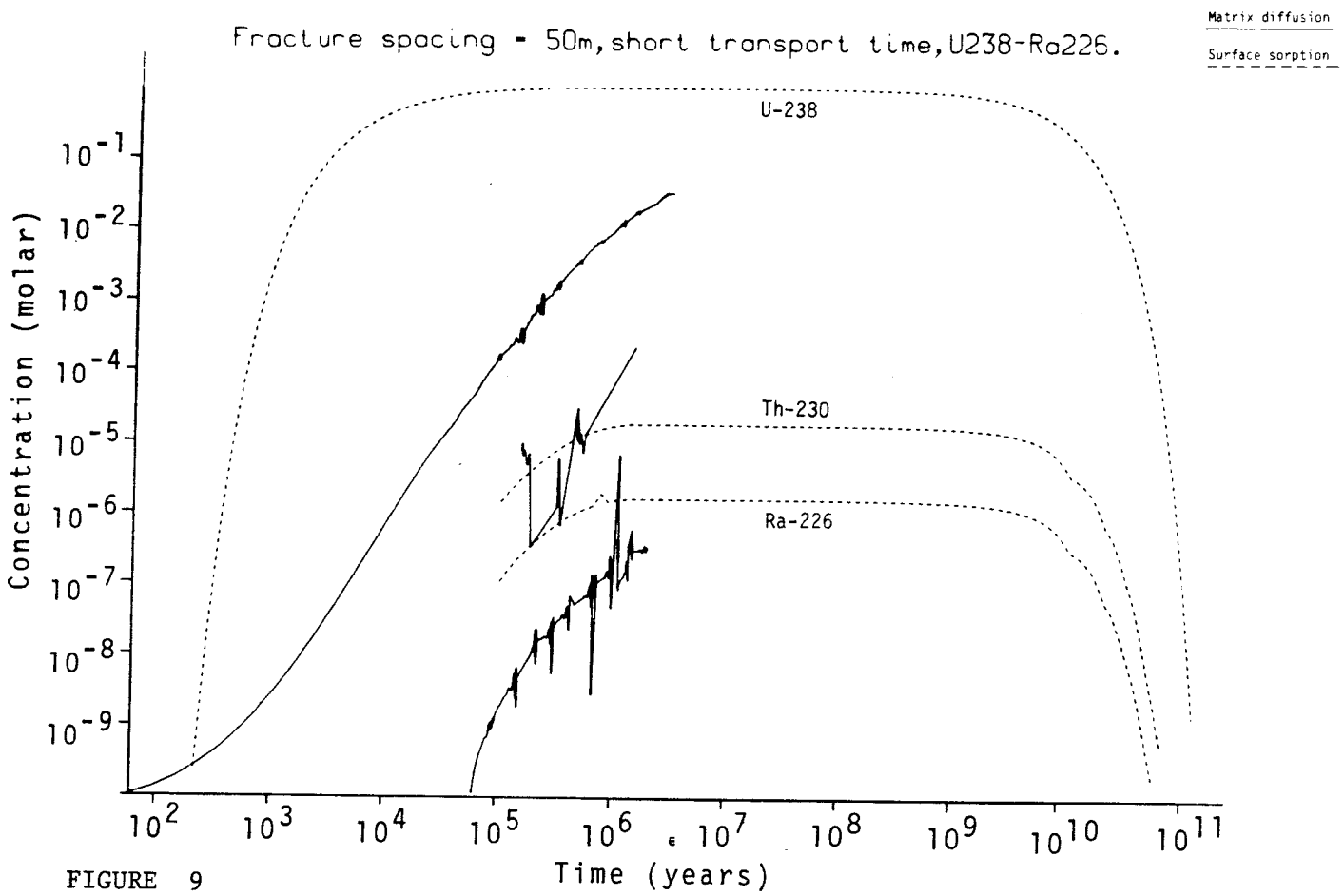

FIGURE 9

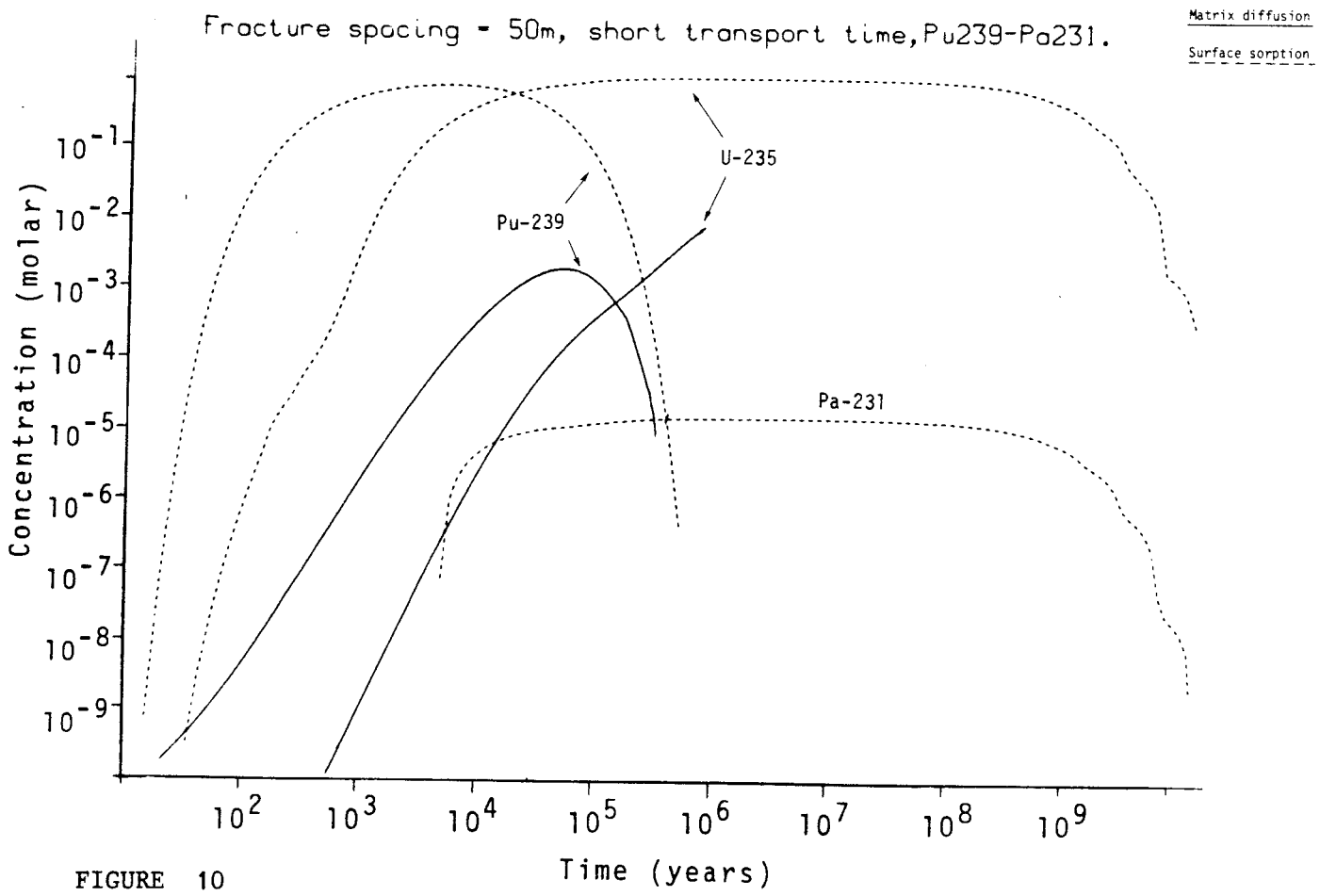

FIGURE 10

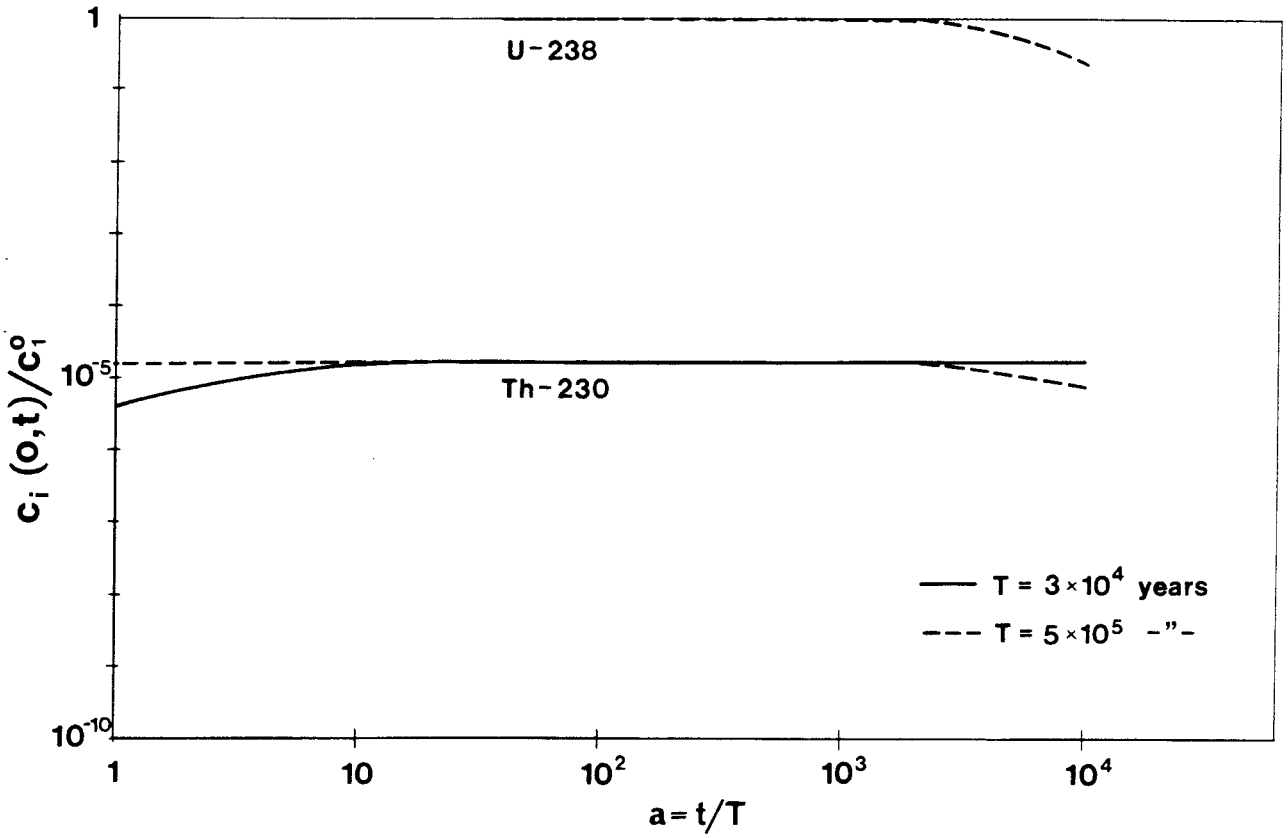

FIGURE 11

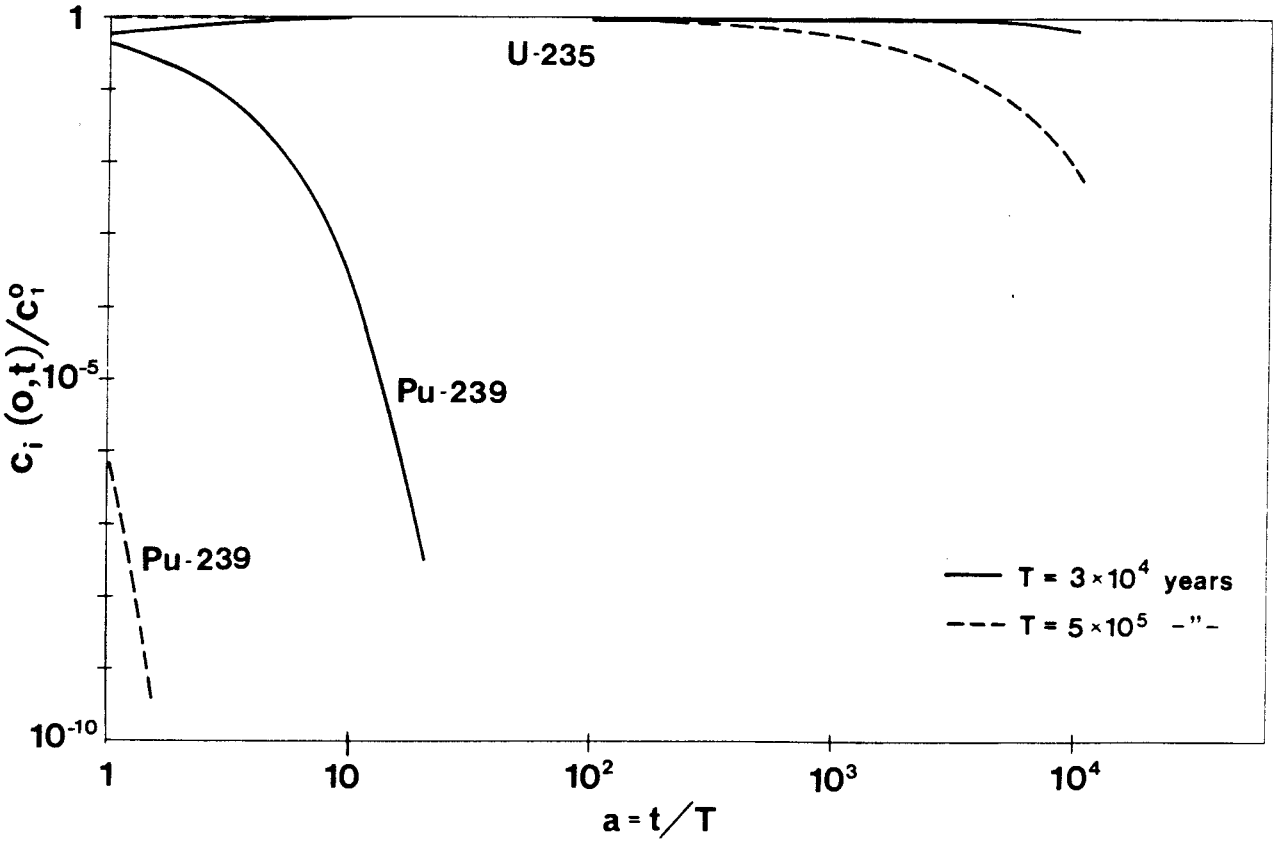

FIGURE 12

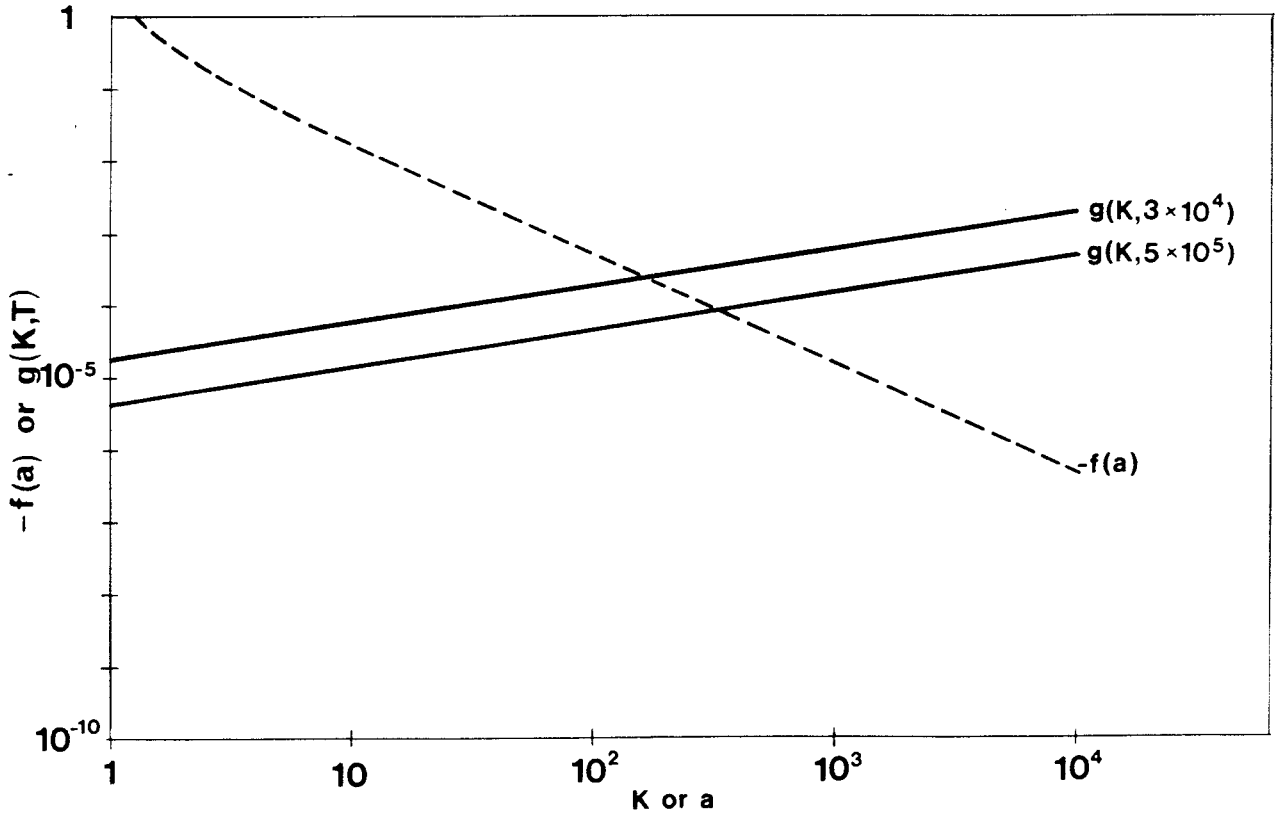
1
10^{-5}
10^{-10}
1
10
10^2
10^3
10^4
K or a
$-f(a)$ or $g(K,T)$
$g(K,3\times10^4)$
$g(K,5\times10^5)$
$-f(a)$

FIGURE 13

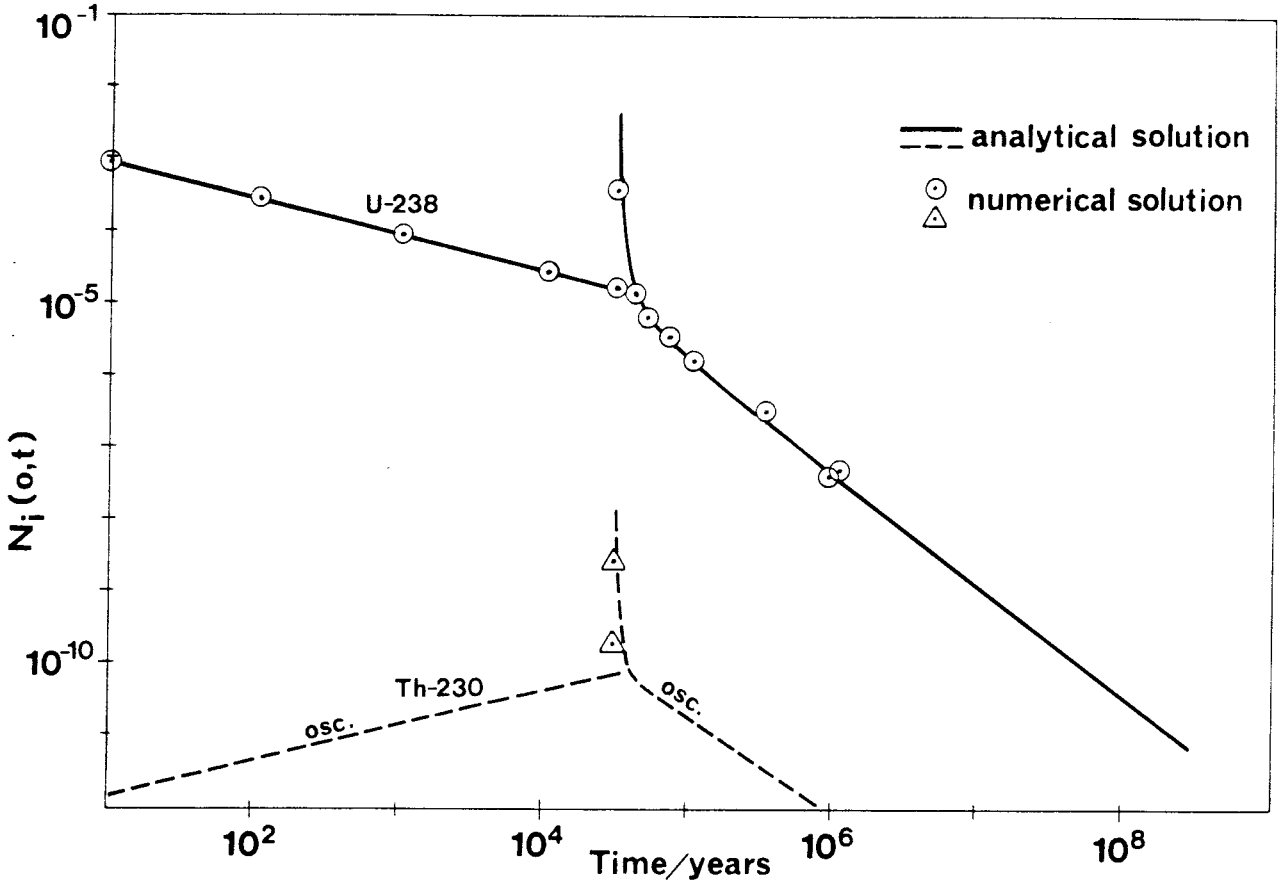

FIGURE 14

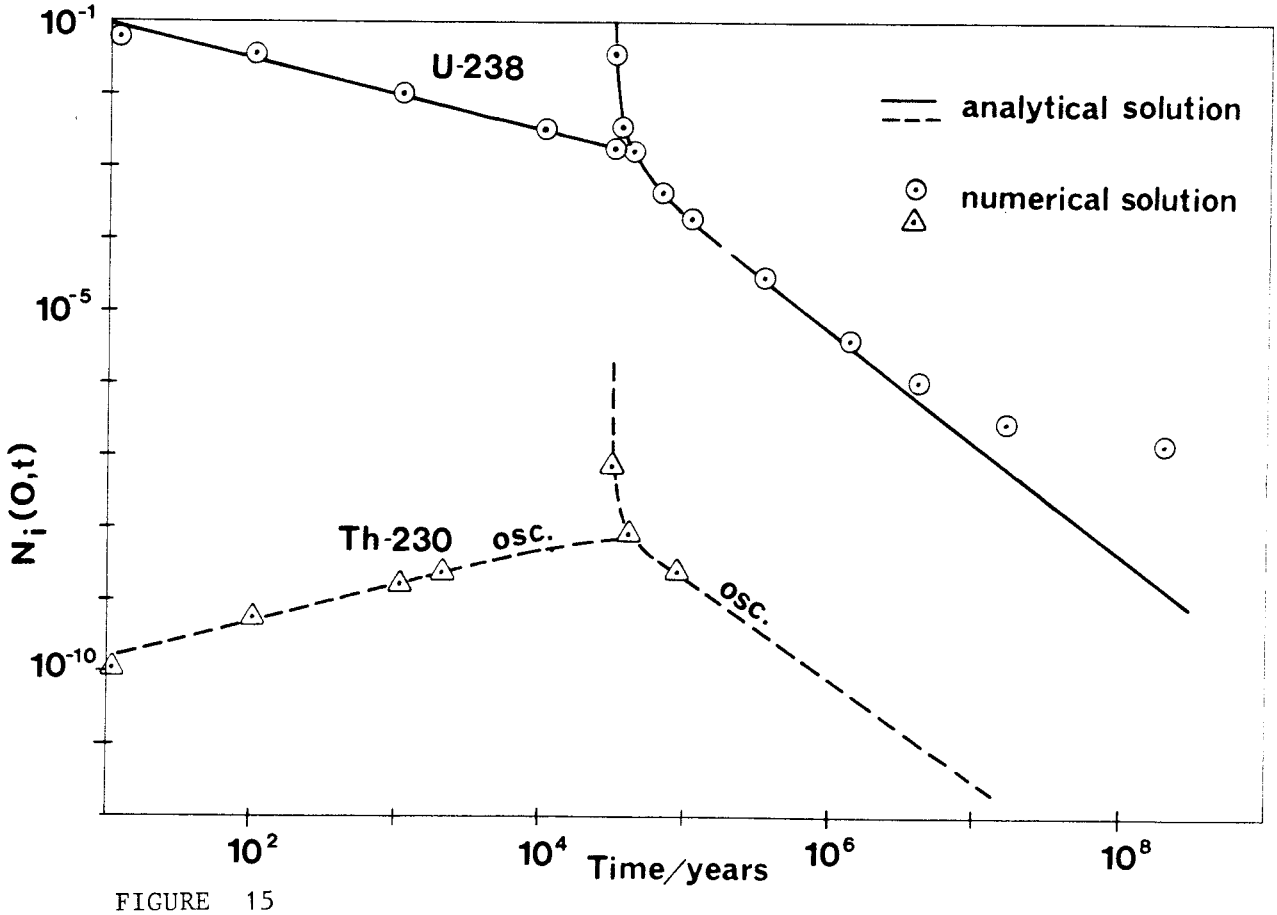

FIGURE 15

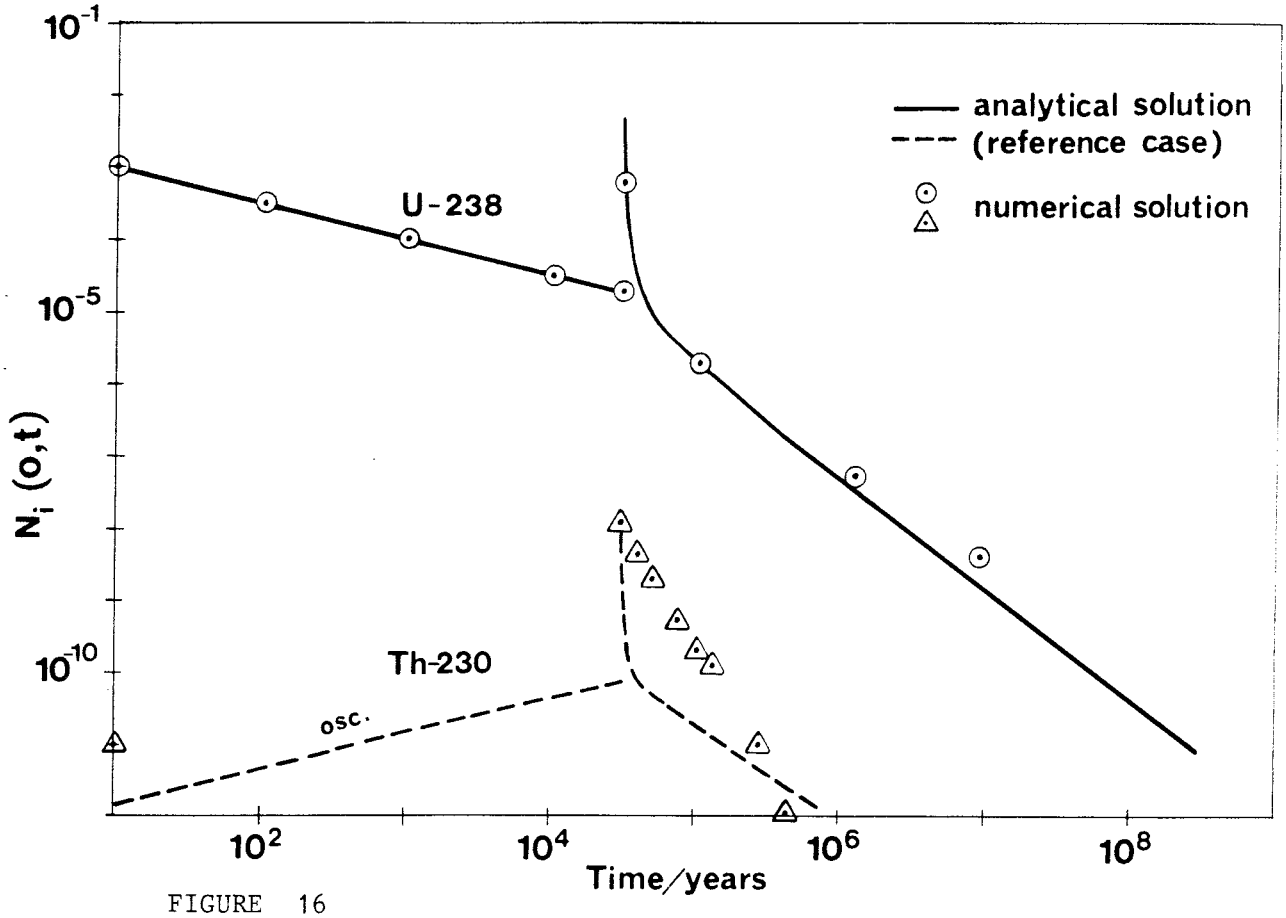

FIGURE 16

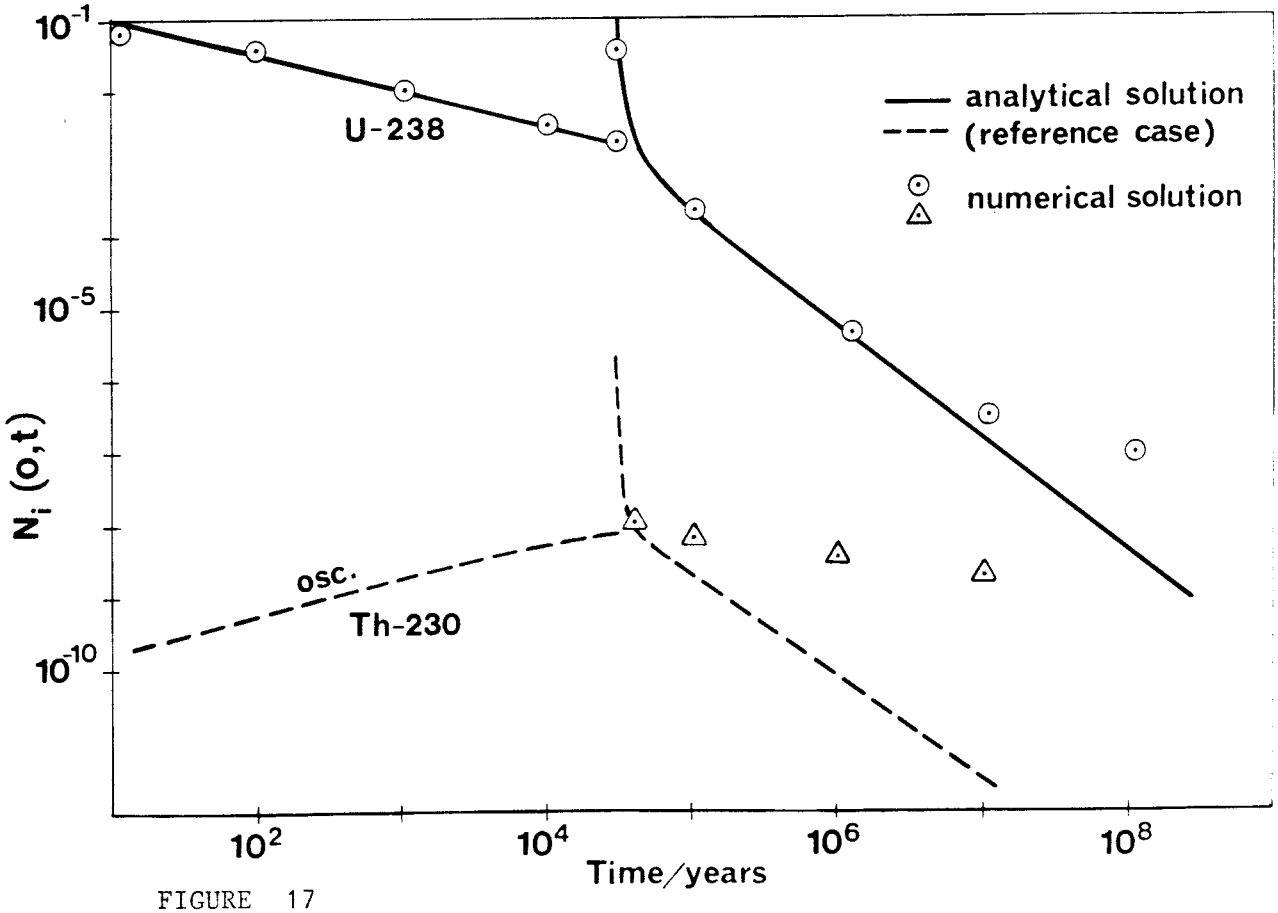

FIGURE 17

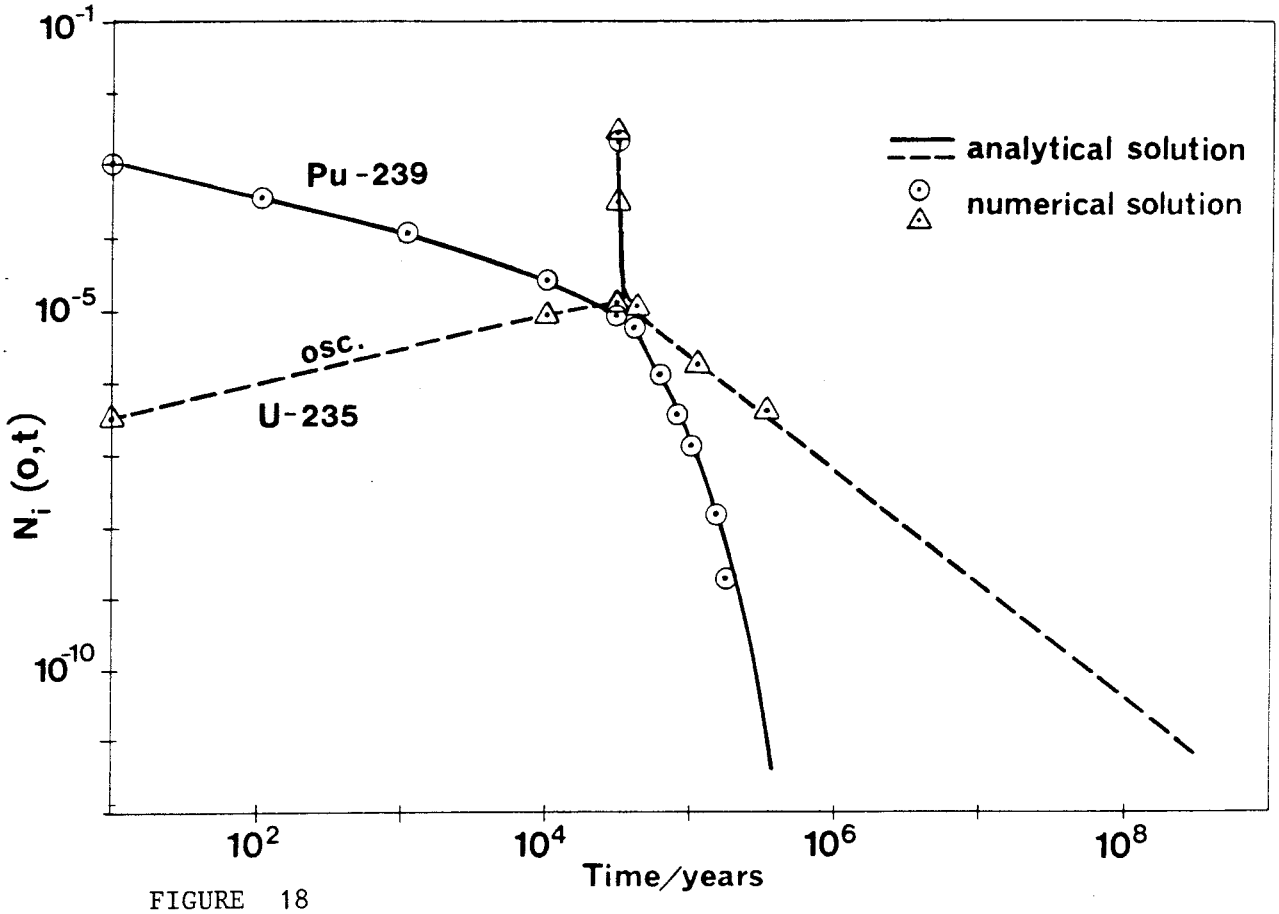

FIGURE 18

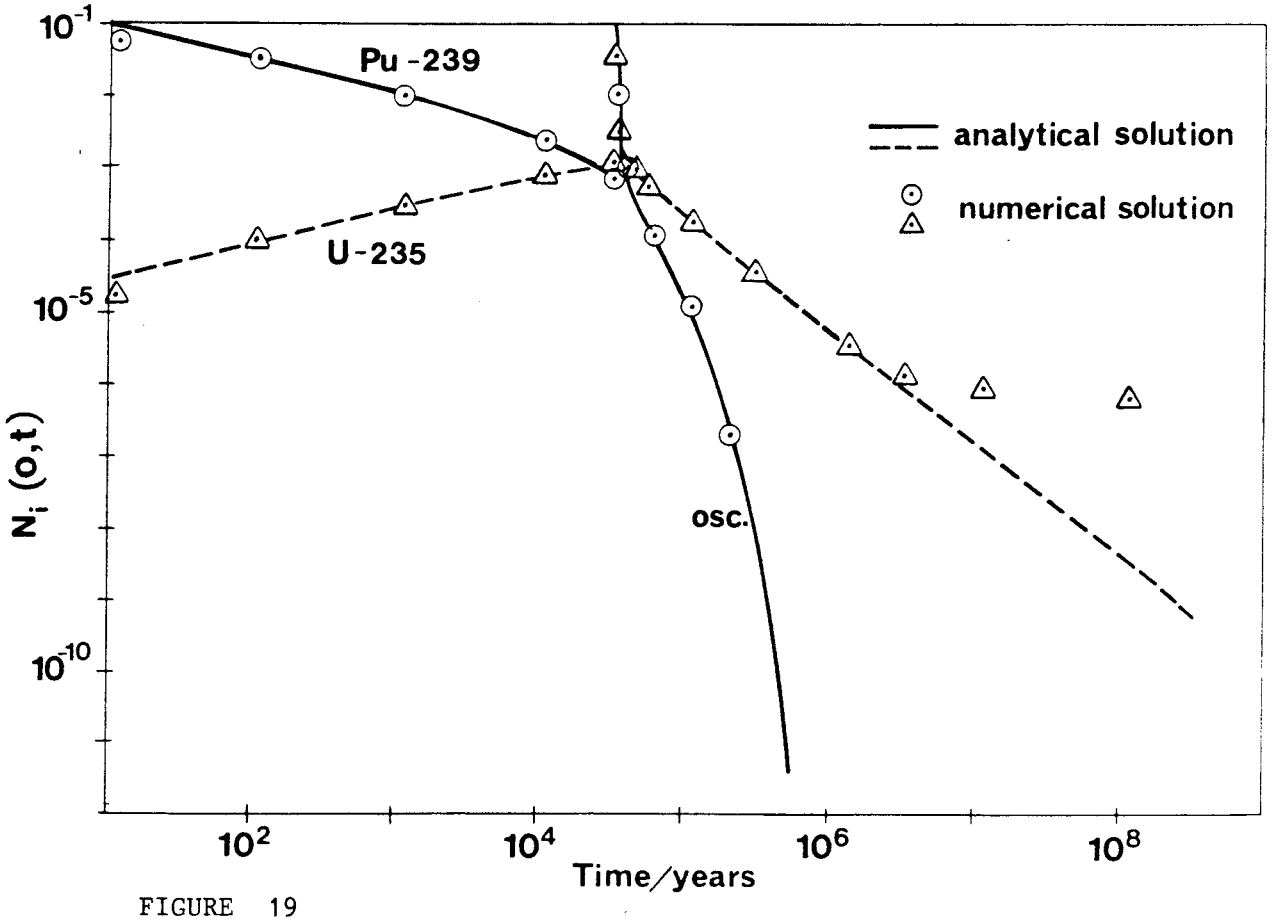

FIGURE 19

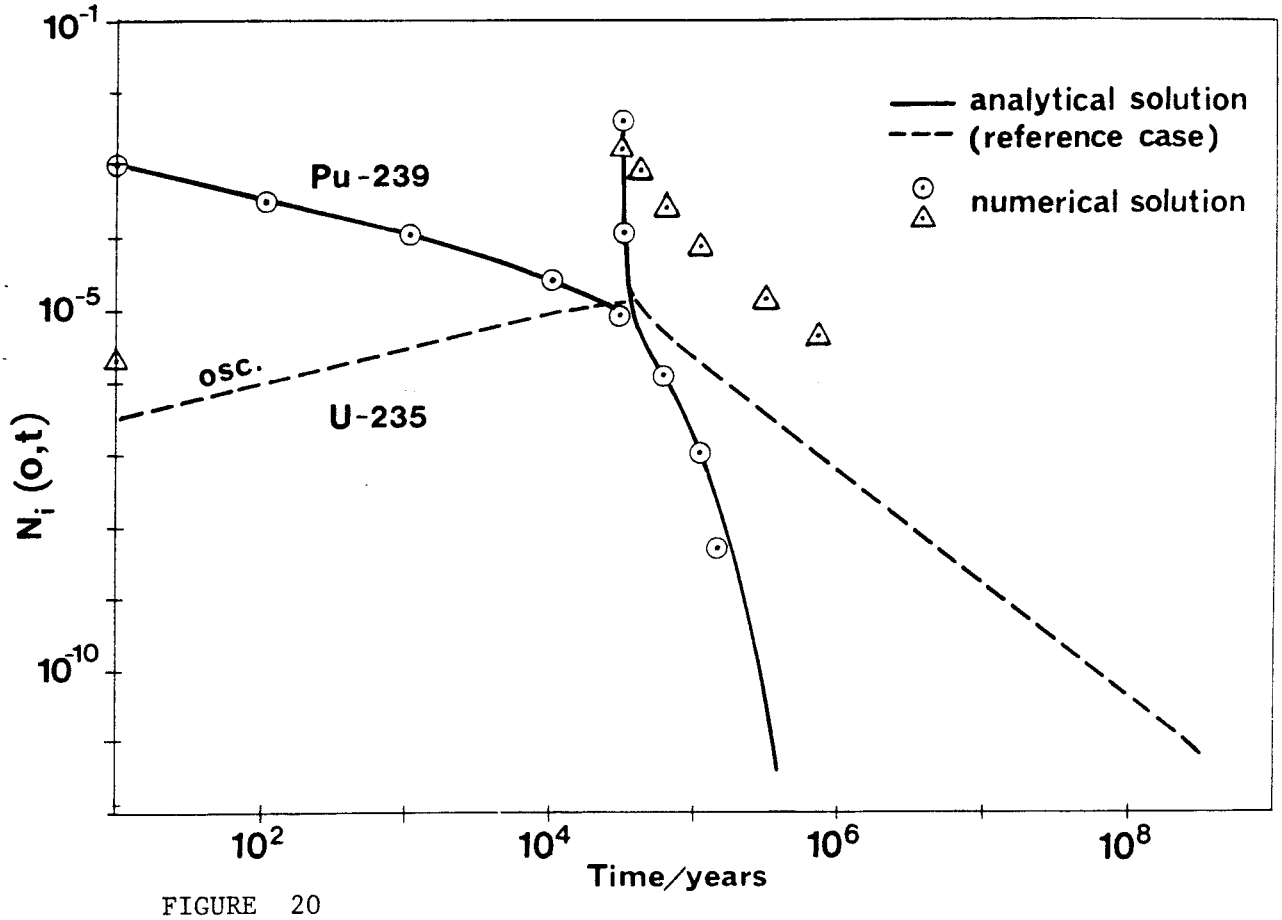

FIGURE 20

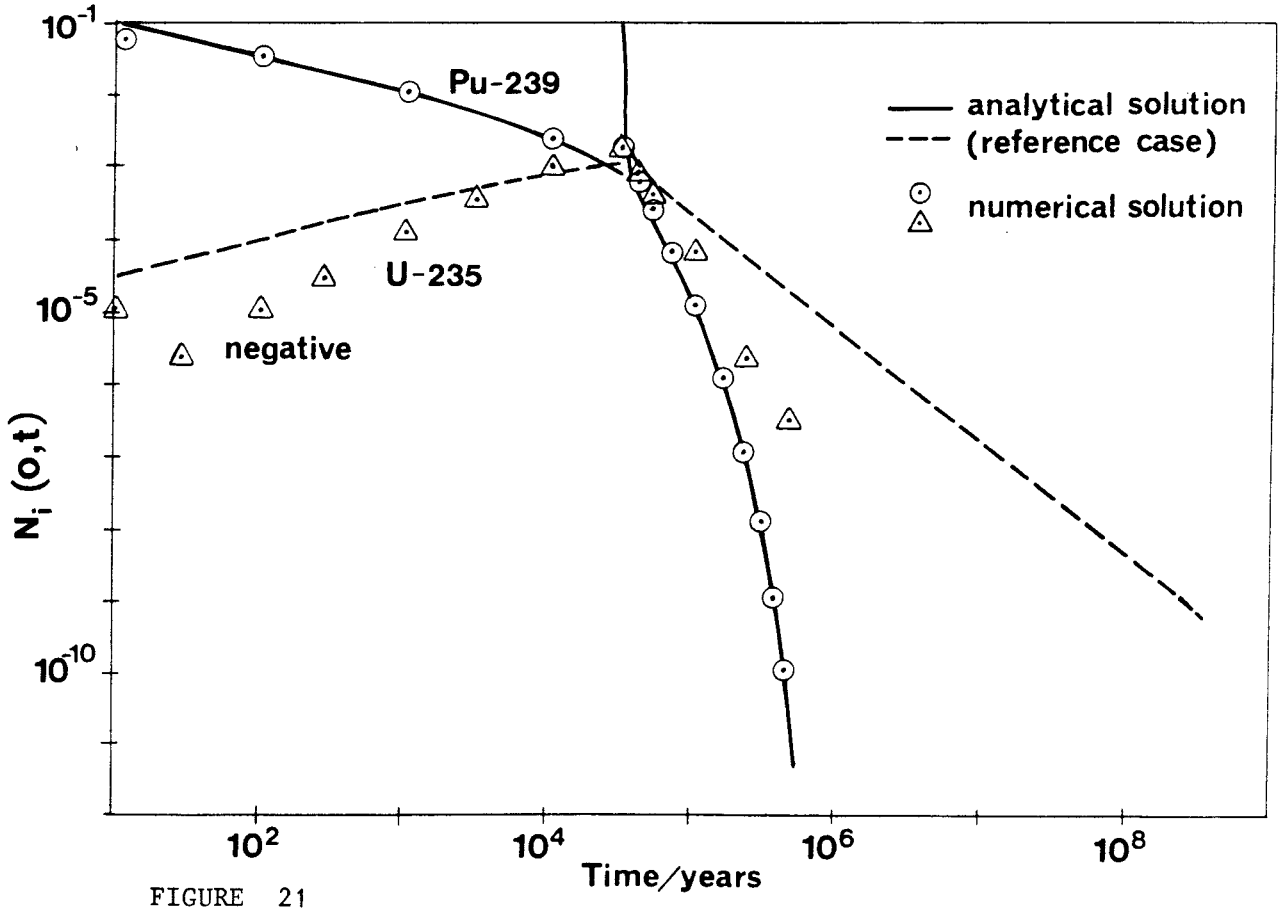

FIGURE 21

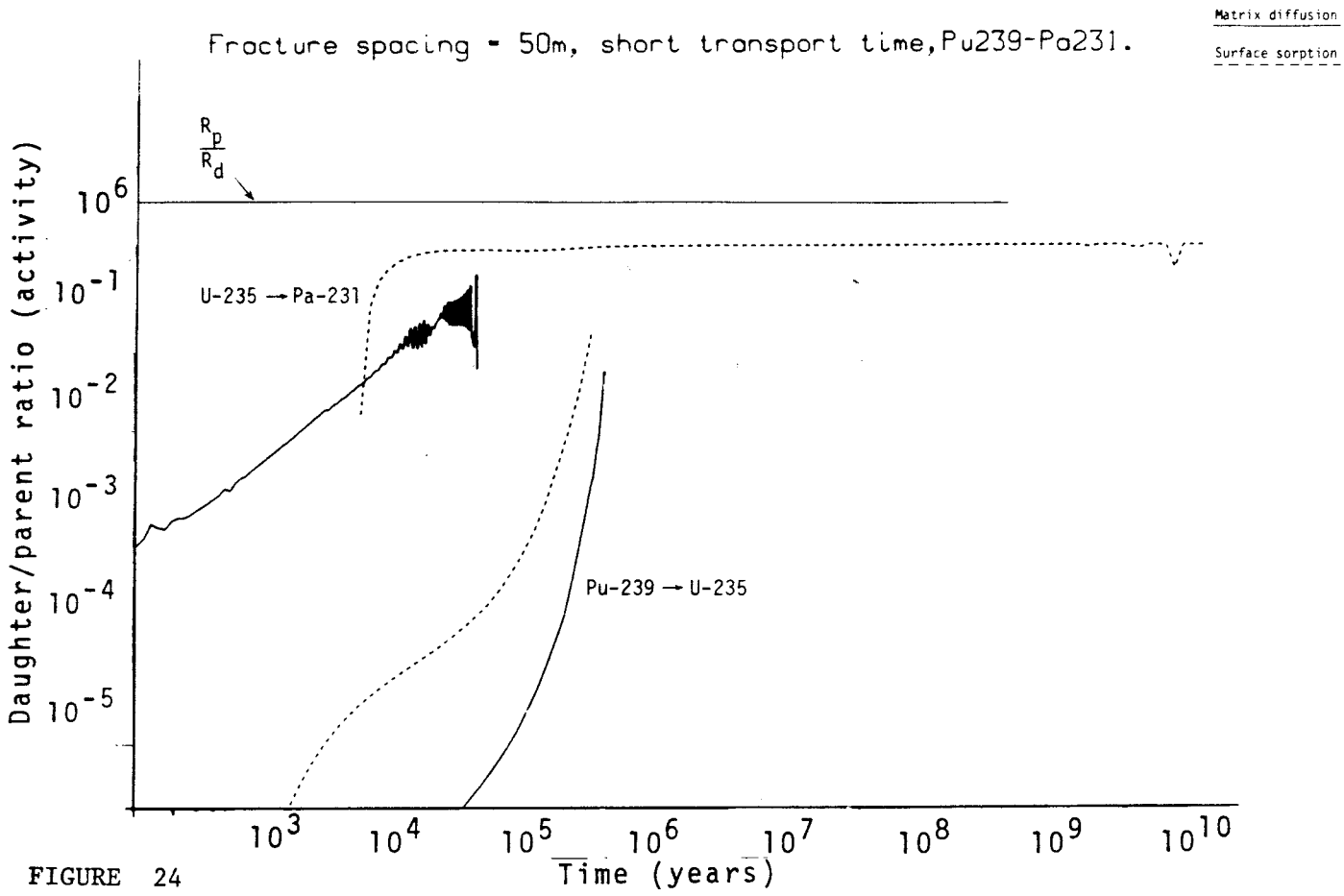

FIGURE 24

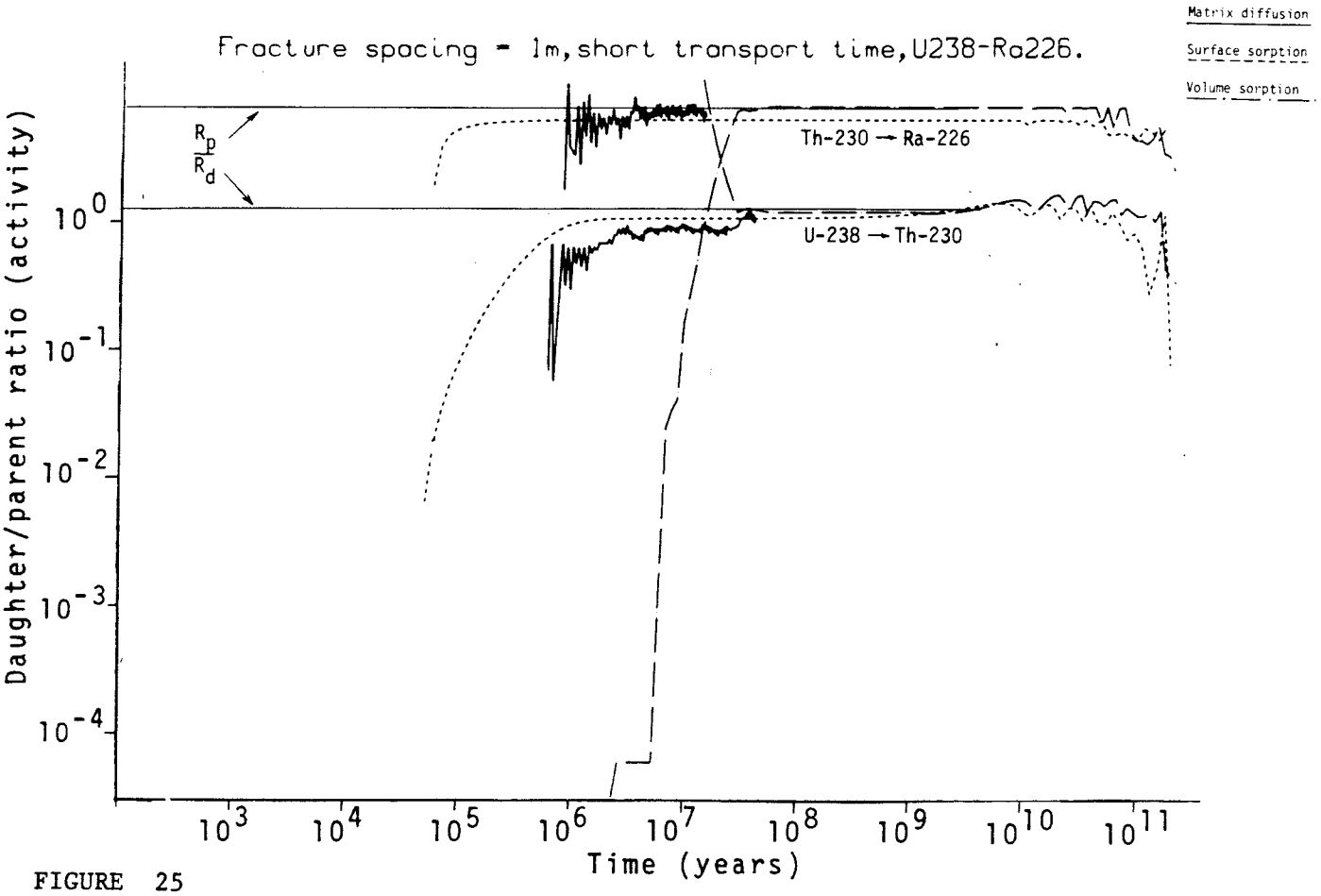

FIGURE 25

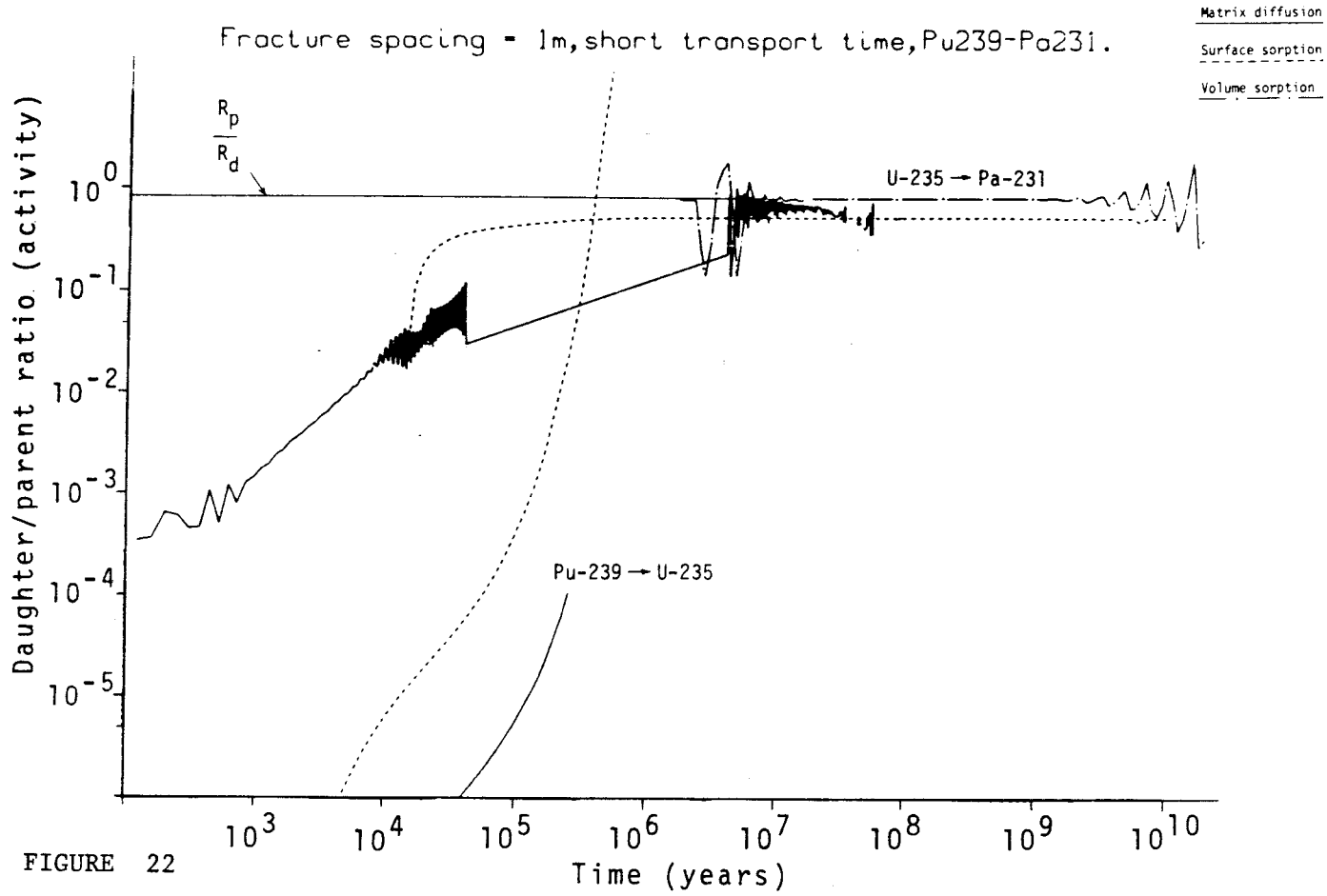

FIGURE 22

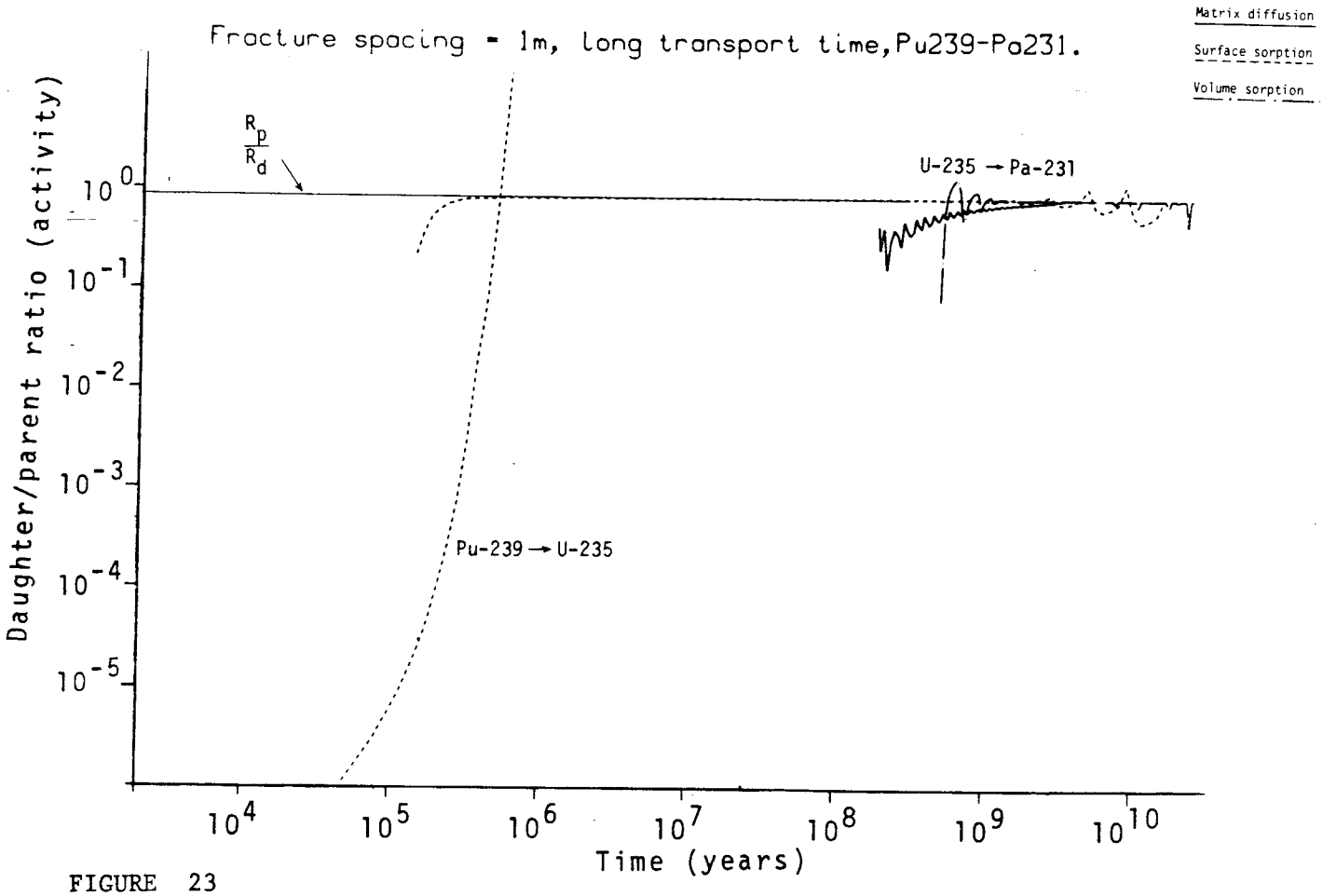

FIGURE 23

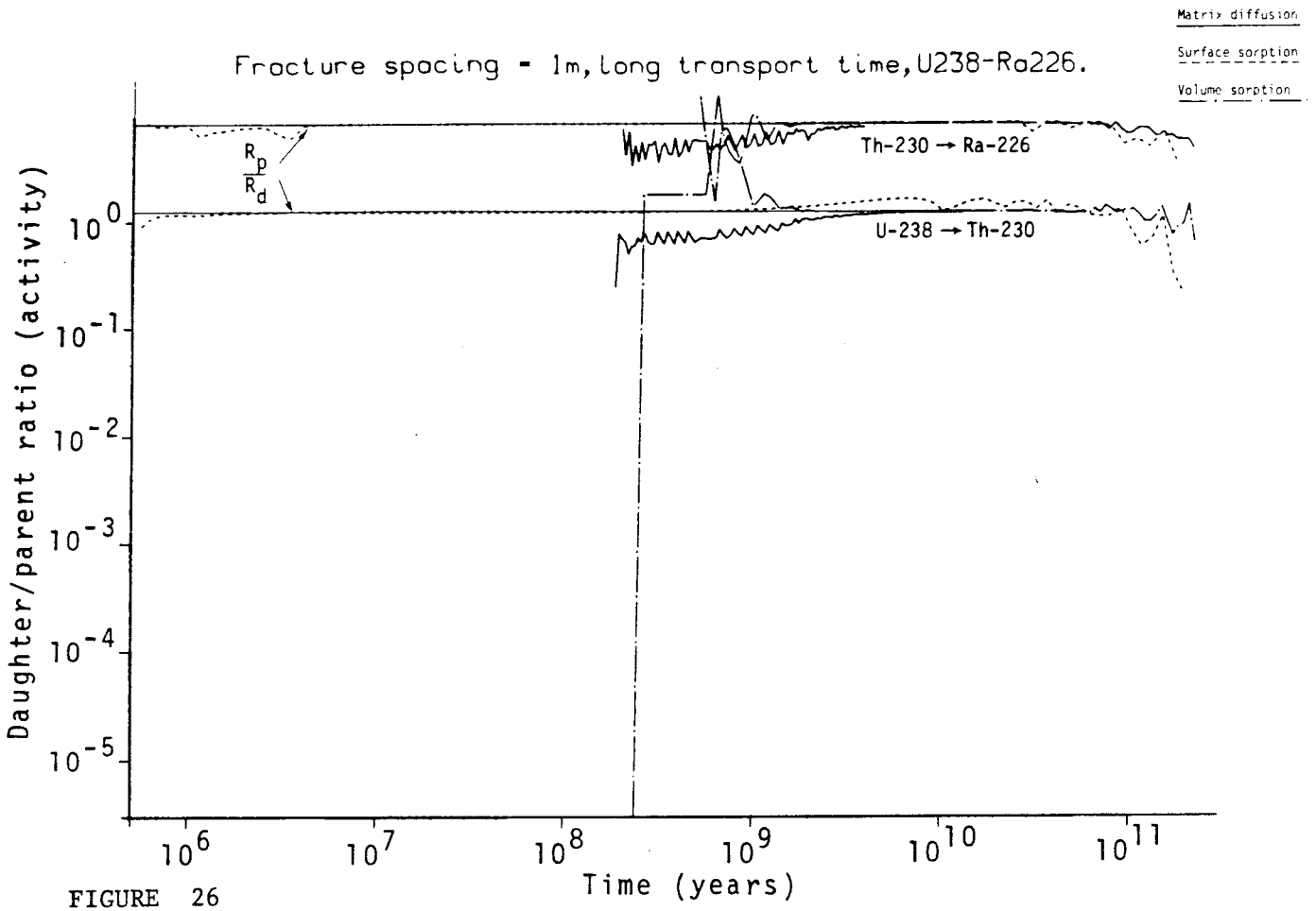

FIGURE 26

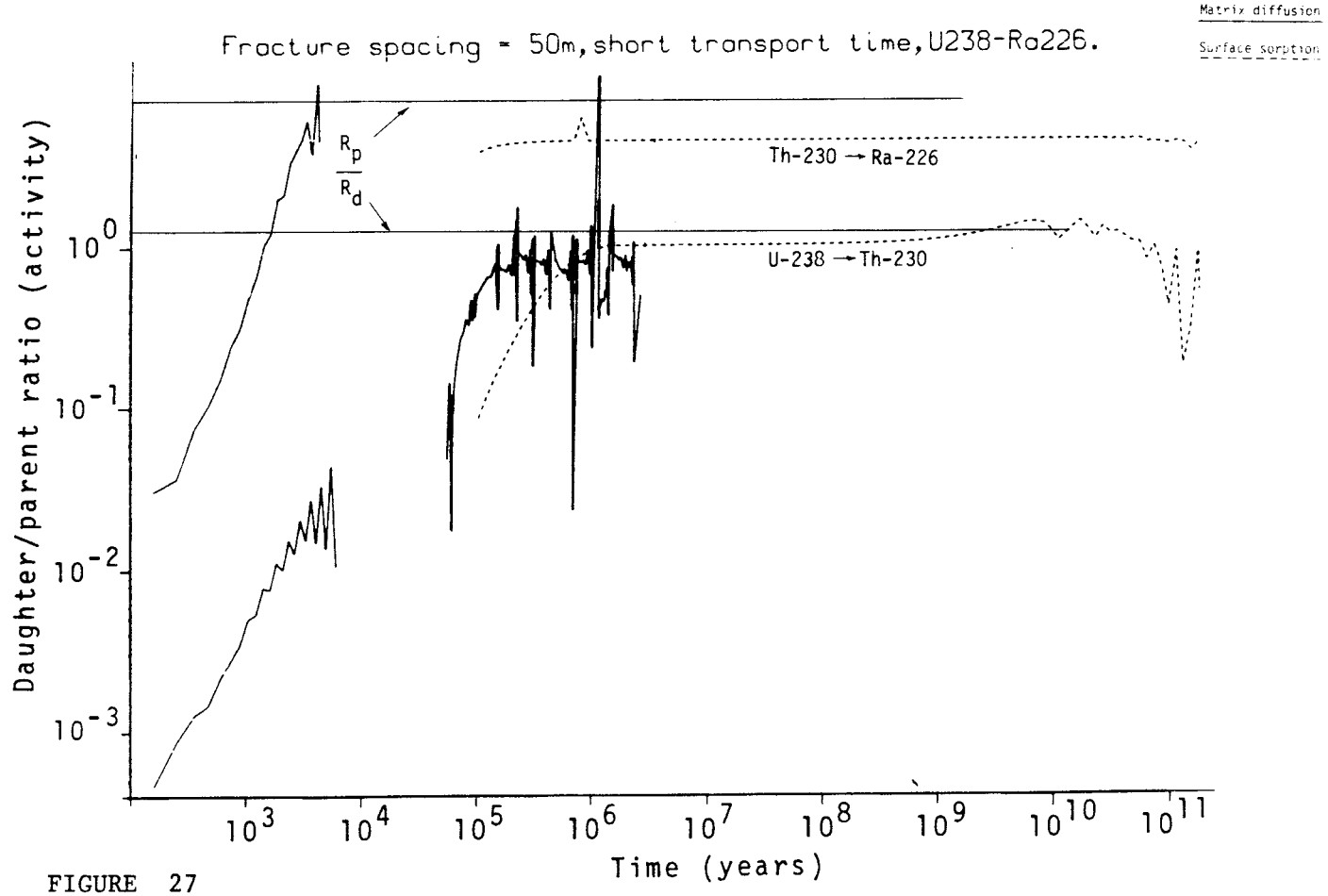

FIGURE 27

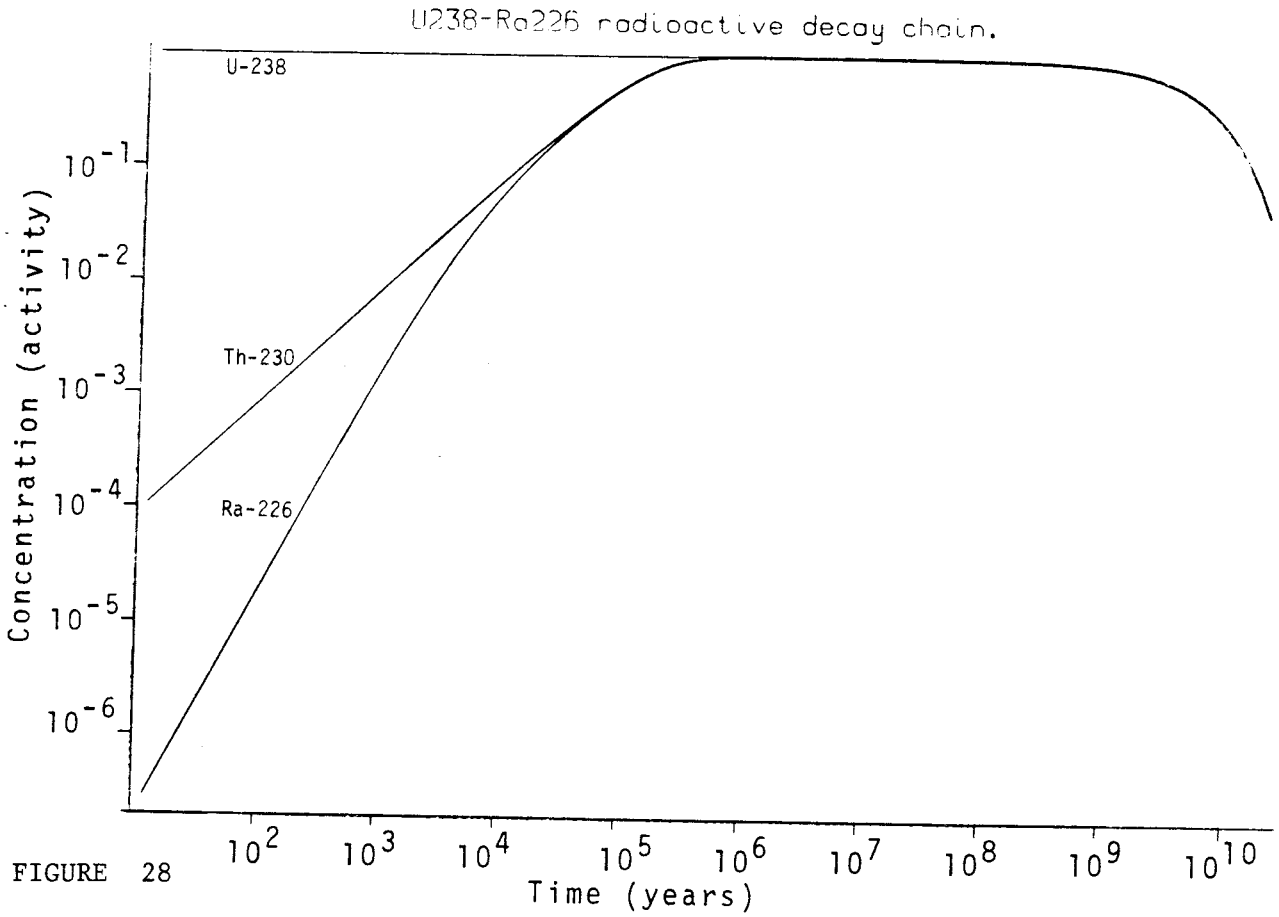

FIGURE 28

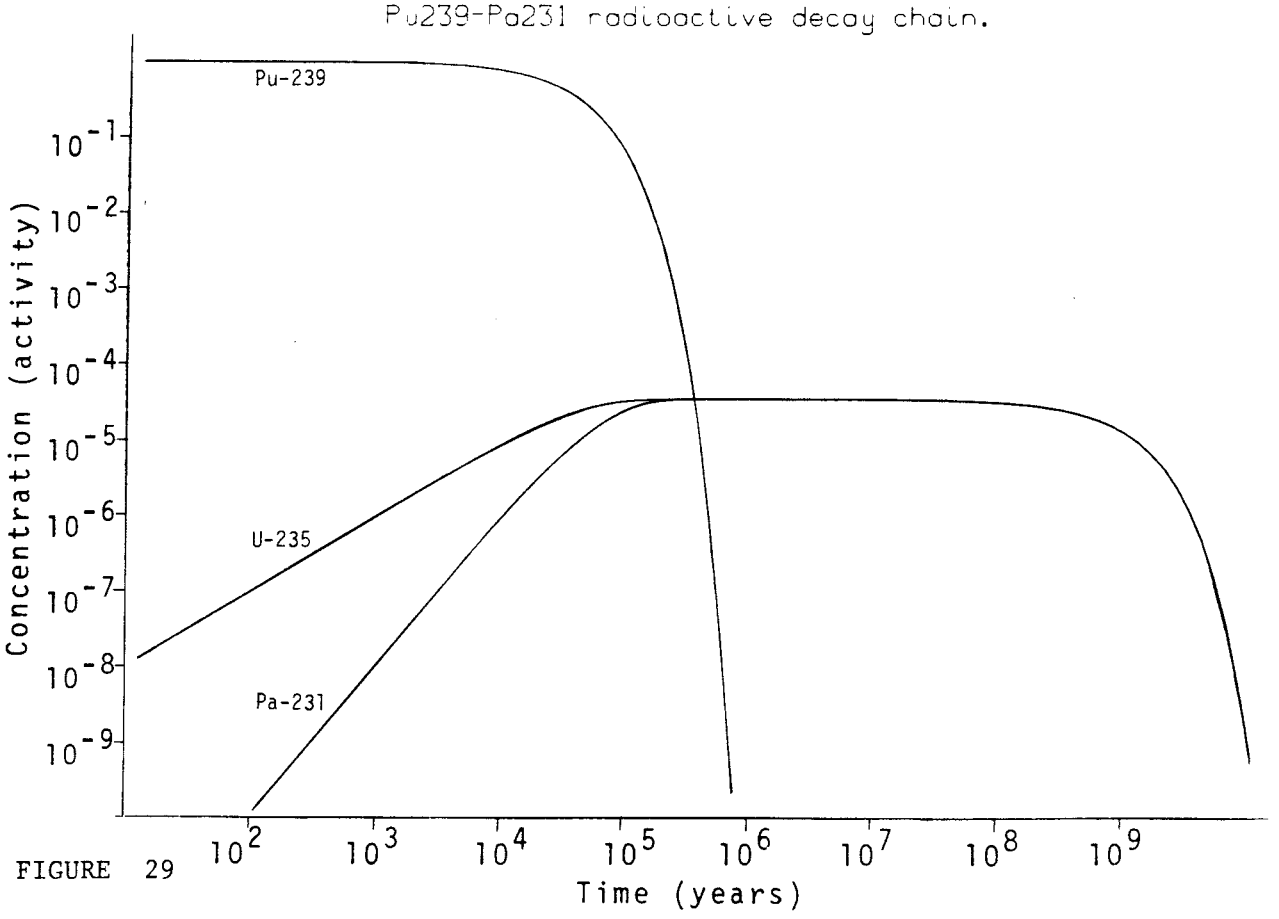

FIGURE 29

FÖRTECKNING ÖVER KBS TEKNISKA RAPPORTER

1977-78

TR 121 KBS Technical Reports 1 - 120.
Summaries. Stockholm, May 1979.

1979

TR 79-28 The KBS Annual Report 1979.
KBS Technical Reports 79-01--79-27.
Summaries. Stockholm, March 1980.

1980

TR 80-26 The KBS Annual Report 1980.
KBS Technical Reports 80-01--80-25.
Summaries. Stockholm, March 1981.

1981

TR 81-17 The KBS Annual Report 1981.
KBS Technical Reports 81-01--81-16
Summaries. Stockholm, April 1982.

1982

TR 82-01 Hydrothermal conditions around a radioactive waste repository
Part 3 - Numerical solutions for anisotropy
Roger Thunvik
Royal Institute of Technology, Stockholm, Sweden
Carol Braester
Institute of Technology, Haifa, Israel
December 1981

TR 82-02 Radiolysis of groundwater from HLW stored in copper canisters
Hilbert Christensen
Erling Bjergbakke
Studsvik Energiteknik AB, 1982-06-29

TR 82-03 Migration of radionuclides in fissured rock:
Some calculated results obtained from a model based on the concept of stratified flow and matrix diffusion
Ivars Neretnieks
Royal Institute of Technology
Department of Chemical Engineering
Stockholm, Sweden, October 1981

TR 82-04 Radionuclide chain migration in fissured rock -
The influence of matrix diffusion
Anders Rasmuson *
Akke Bengtsson **
Bertil Grundfelt **
Ivars Neretnieks *
April, 1982

* Royal Institute of Technology
Department of Chemical Engineering
Stockholm, Sweden

** KEMAKTA Consultant Company
Stockholm, Sweden

TR 82-05 Migration of radionuclides in fissured rock -
Results obtained from a model based on the concepts of hydrodynamic dispersion and matrix diffusion
Anders Rasmuson
Ivars Neretnieks
Royal Institute of Technology
Department of Chemical Engineering
Stockholm, Sweden, May 1982

TR 82-06 Numerical simulation of double packer tests
Calculation of rock permeability
Carol Braester
Israel Institute of Technology, Haifa, Israel
Roger Thunvik
Royal Institute of Technology
Stockholm, Sweden, June 1982

TR 82-07 Copper/bentonite interaction
Roland Pusch
Division Soil Mechanics, University of Luleå
Luleå, Sweden, 1982-06-30

TR 82-08 Diffusion in the matrix of granitic rock
Field test in the Stripa mine
Part 1
Lars Birgersson
Ivars Neretnieks
Royal Institute of Technology
Department of Chemical Engineering
Stockholm, Sweden, July 1982